Department of Biotechnology and Chemical Technology

Molecular interactions of hydrophobin proteins with their surroundings

Mathias S. Grunér

Aalto University

DOCTORAL DISSERTATIONS

Aalto University publication series
DOCTORAL DISSERTATIONS 206/2015
VTT SCIENCE 114

Molecular interactions of hydrophobin proteins with their surroundings

Mathias S. Grunér

A doctoral dissertation completed for the degree of Doctor of Science (Technology) to be defended, with the permission of the Aalto University School of Chemical Technology, at a public examination held at the lecture hall KE2 at the Aalto University School of Chemical Technology (Espoo, Finland) on the 10th of December 2015, at 12 o'clock noon.

Aalto University
School of Chemical Technology
Department of Biotechnology and Chemical Technology
Biomolecular materials

Supervising professors
Professor Markus B. Linder
Aalto University, Finland

Thesis advisors
Professor Markus B. Linder
Aalto University, Finland

Preliminary examiners
Professor Ewa Rogalska
University of Lorraine, France

Professor Paola Giardina
Universitario Monte S. Angelo, Italy

Opponents
Professor Guy Derdelinckx
KU Leuven, Belgium

Aalto University publication series
DOCTORAL DISSERTATIONS 206/2015

VTT SCIENCE 114

ISBN 978-952-60-6556-4 (printed)
ISBN 978-952-60-6557-1 (pdf)
ISSN-L 1799-4934
ISSN 1799-4934 (printed)
ISSN 1799-4942 (pdf)
http://urn.fi/URN:ISBN:978-952-60-6557-1

ISBN 978-951-38-8367-6 (printed)
ISBN 978-951-38-8366-9 (pdf)
ISSN-L 2242-119X
ISSN 2242-119X (printed)
ISSN 2242-1203 (pdf)
http://urn.fi/URN:ISBN:978-951-38-8366-9

Unigrafia Oy
Helsinki 2015

Finland

441 697
Printed matter

Author
Mathias S. Grunér

Name of the doctoral dissertation
Molecular interactions of hydrophobin proteins with their surroundings

Publisher School of Chemical Technology

Unit Department of Biotechnology and Chemical Technology

Series Aalto University publication series DOCTORAL DISSERTATIONS 206/2015

Field of research Biotechnology

Manuscript submitted 5 June 2015 **Date of the defence** 10 December 2015

Permission to publish granted (date) 6 November 2015 **Language** English

☐ **Monograph** ☒ **Article dissertation (summary + original articles)**

Abstract

This thesis describes the properties of a group of proteins named hydro-phobins, which fulfil a variety of functions in the growth and function of filamentous fungi. Hydrophobins can be utilized as coatings/protective agents, in adhesion, in surface modifications and overall functions that require surfactant-like properties. This work is concentrated on the hydrophobins HFBI,
HFBII and HFBIII expressed by Trichoderma reesei. The aims of this study were to examine in what manner hydrophobins function when interacting with their surroundings and how their surroundings affect their function.
Hydrophobins were shown strongly to adhere to surfaces of varying polarity and structure by self-assembly, governed by their amphiphilic nature, and to adsorb with different orientation on hydrophilic and hydrophobic surfaces. The proteins were shown to selectively recruit other proteins and molecules to a self-assembled amphiphilic film of hydrophobin. HFBI variants bound to a surface were shown to recruit T. reesei enzymes specifically depending on localized protein surface charge on the hydrophilic part of the protein, and HFBII adsorbed on nanoparticles was shown to bind layers of human plasma proteins in different manner when adsorbed on nanoparticles of varying polarity. Surface films formed by hydrophobins were shown to be highly elastic, and charged residues on the side of the proteins were shown to have a role in stabilizing the protein films formed. The surroundings in which the proteins exist were shown to also affect their function. Surfaces of varying polarity in the protein surroundings affected how they self-assemble, and hydrophobin multimer exchange in solution was shown to be governed by hydrophobic interactions and the multimer exchange behaviour was shown to be affected by other proteins and molecules. HFBII and HFBI were shown to interact in solution, altering multimer kinetics and thermodynamics considerably.
Solution association methods, surface characterization analysis methods and size measurement techniques such as stopped-flow spectroscopy, quartz crystal microbalance with dissipation and differential centrifugal sedimentation were used.
The results presented here show that hydrophobins function by selectively interacting with their surroundings assembled at various interfaces specifically recruiting other proteins and molecules and that the surroundings in which the proteins exist also affects their function in terms of multimer exchange behaviour and surface adhesion properties. The knowledge learned here regarding hydrophobins, show that these proteins can be specialized to function as highly selective self-assembling building blocks in applications such as biosensors and biocompatible coatings, and gives new insight in the growth and function of filamentous fungi.

Keywords Hydrophobin, self-assembly, HFBI, HFBII, adhesion

ISBN (printed) 978-952-60-6556-4 **ISBN (pdf)** 978-952-60-6557-1

ISSN-L 1799-4934 **ISSN (printed)** 1799-4934 **ISSN (pdf)** 1799-4942

Location of publisher Helsinki **Location of printing** Helsinki **Year** 2015

Pages 110 **urn** http://urn.fi/URN:ISBN:978-952-60-6557-1

Författare
Mathias S. Grunér

Doktorsavhandlingens titel
Molecular interactions of hydrophobin proteins with their surroundings

Utgivare Högskolan för kemiteknik

Enhet Institutionen för bio- och kemiteknik

Seriens namn Aalto University publication series DOCTORAL DISSERTATIONS 206/2015

Forskningsområde Bioteknik

Inlämningsdatum för manuskript 05.06.2015 **Datum för disputation** 10.12.2015

Beviljande av publiceringstillstånd (datum) 06.11.2015 **Språk** Engelska

☐ **Monografi** ☒ **Sammanläggningsavhandling (sammandrag plus separata artiklar)**

Sammandrag

Denna avhandling beskriver egenskaperna av en grupp proteiner kallade hydrofobiner, vilka utför en rad viktiga funktioner i fråga om tillväxt och funktion av filamentösa svampar. Hydrofobiner kan användas som skyddade lager och beläggningar, i adhesion, ytmodifiering och allmänt där ytaktivitet är av vikt. Detta arbete fokuserar på hydrofobinerna HFBI, HFBII och HFBIII uttryckta av Trichoderma reesei. Målen med arbetet var att undersöka hydrofobiners funktion att interagera med sin omgivning och hur omgivningen i sin tur påverkar hydrofobinernas funktion.

Hydrofobiner påvisades att starkt fästa till ytor av varierande polaritet och struktur genom självorganisering drivna av sin amfifila natur, och att adsorbera med skild orientering på hydrofila respektive hydrofoba ytor. Resultaten visade även att proteinerna selektivt kan rekrytera andra proteiner till en självorganiserad film av hydrophobin. Muterade varianter av HFBI bundna till en yta påvisades att rekrytera enzymer av T. reesei beroende på lokala laddningar på den hydrofila delen av proteinets yta, och HFBII adsorberat på nanopartiklar band till sig humana plasmaproteiner i lager med olika sammansättning och typ beroende polaritet av nanopartikel. Hydrofobinfilmer formade på ytor konstaterades även vara mycket elastiska, och laddade sidokedjor på sidan proteinet verkar stabiliserande på hydrofobinfilmen. Omgivningen i vilken hydrofobinerna verkar konstaterades att påverka deras funktion. Ytor av varierande polaritet i proteinernas omgivning påverkar hur de självorganiserar. Utbyte av hydrofobinmultimerer i lösning påvisades vara styrt av hydrofoba interaktioner och multimerutbytet påverkas av andra proteiner och molekyler. HFBI och HFBII konstaterades interagera i lösning vilket i hög grad påverkade kinetiken och termodynamiken av multimerutbytetet.

Lösningsassocieringsmetoder, ytkarakteriseringsanalysmetoder och storleksanalystekniker som stopped-flow spektroskopi, QCM-D (Quartz crystal microbalance with dissipation) och DCS (differential centrifugal sedimentation) användes.

Resultaten av detta arbete visar att hydrofobiner verkar genom att selektivt interagera med sin omgivning, ordnade vid olika gränsytor, där de specifikt rekryterar olika proteiner och molekyler, samt att omgivingen där proteinerna uppträder även påverkar hydrofobinernas funktion i termer av multimerutbyte i lösning och ytadhesionsegenskaper. Kunskapen som förvärvats i detta arbete rörande hydrofobiner visar att dessa proteiner kan specialiseras för att fungera som ytterst selektiva självorganiserande byggklossar för applikationer som t.ex. biosensorer och biokompatibla beläggningar, samt ger ny insikt i tillväxt och funktion av filamentösa svampar.

Nyckelord Hydrophobin, self-assembly, HFBI, HFBII, adhesion

ISBN (tryckt) 978-952-60-6556-4	**ISBN (pdf)** 978-952-60-6557-1	
ISSN-L 1799-4934	**ISSN (tryckt)** 1799-4934	**ISSN (pdf)** 1799-4942
Utgivningsort Helsingfors	**Tryckort** Helsingfors	**År** 2015
Sidantal 110	**urn** http://urn.fi/URN:ISBN:978-952-60-6557-1	

Acknowledgements

Starting in autumn 2010 I got the chance to perform my master thesis in the guidance of Professor Markus Linder at the VTT Nanobiomaterials group. I was at an early stage inspired by the creative possibilities of the field and by the opportunity to work with such talented people. My work of the fascinating hydrophobin proteins continued as thesis work in the same group from September 2011 until November 2012.

There are numerous people whom I wish to acknowledge for their valuable contributions and for making this thesis possible.

I express my deepest gratitude to my thesis supervisor Professor Markus Linder for his support, encouragement, patience and for always finding time for discussions, meetings and questions. I want to thank Dr. Géza Szilvay for educating and supporting me, and for introducing me to the world of science in the best way possible. I also want to thank Dr. Michael Lienemann for his kind support and for useful discussions, especially during the later stages of my research.

I thank the technology managers Dr. Raija Lantto and Dr. Niklas von Weymarn for the great working facilities. I acknowledge the School of Chemical Technology, Aalto University for the possibility to perform my doctoral degree. The National graduate school in informational and structural biology and the director Professor Mark Johnson are thanked for financial support.

Dr. Riitta Partanen is thanked for being an excellent and inspiring team leader. Dr. Arja Paananen is thanked for her advice, interesting scientific discussions and guidance in experiments. Riitta Suihkonen is appreciated for practical advice in the laboratory and for all discussions, especially in Finnish.

At University College Dublin, Professor Kenneth Dawson is thanked for accepting me as a guest researcher in his group and Dr. Marco Monopoli for his continuous support, guidance and inspiration.

I also would like to thank my colleagues, Jani-Markus, Jaana, Suvi, Päivi, Evi, Timo, Bartosz and Roberto and all other members of the Nanobiomaterials group for practical support and for creating a warm work atmosphere, as well as my other colleagues at VTT Biotechnology, Greta, Wesley, Georg, Ronny and Harry for inspiring discussions.

I would like to especially thank my family for their interest, participation and fantastic support, for always encouraging me to move forward and to trust my intuition and for always finding time to listen to my thoughts and reflections.

Mariehamn 12.11.2015

Mathias S. Grunér

Contents

List of Abbreviations and Symbols

AFM	Atomic force microscopy
DCS	Differential centrifugal sedimentation
DLS	Dynamic light scattering
Ea	Activation energy
FRET	Förster resonance energy transfer
HC	Hard corona
IS	*In situ* corona
LB	Langmuir-Blodgett
NP	Nanoparticle
QCM-D	Quartz crystal microbalance with dissipation
SAM	Self-assembled monolayer
SEC	Size exclusion chromatography
SDS-PAGE	Polyacrylamide gel electrophoresis using sodium dodecyl sulfate
SF	Stopped-Flow spectroscopy
$t_{1/2}$	Half-life
WCA	Water contact angle

List of Publications

This doctoral dissertation consists of a summary and of the following publications which are referred to in the text by their numerals

I. Grunér, Mathias S; Kauscher, Ulrike; Linder, Markus B; Monopoli, Marco P. An environmental route of exposure affects the formation of nanoparticle coronas in blood plasma. Accepted for publication in the journal Journal of Proteomics, Elsevier B.V. in the year 2015

II. Lienemann, Michael; Grunér, Mathias S; Paananen, Arja; Siika-Aho, Matti; Linder, Markus B; 2015. Charge-Based Engineering of Hydrophobin HFBI: Effect on Interfacial Assembly and Interactions. ACS Publications. Biomacromolecules, volume 16, issue 4, pages 1283-1292. ISSN 1526-4602.DOI: 10.1021/acs.biomac.5b00073

III. Grunér, Mathias S; Szilvay, Géza R; Berglin, Mattias; Lienemann, Michael; Laaksonen, Päivi; and Linder, Markus B. 2012. Self-assembly of Class II Hydrophobins on Polar Surfaces. American Chemical Society. Langmuir, volume 28, issue 9, pages 4293–4300. ISSN 0743-7463. DOI:10.1021/la300501u

IV. Grunér, Mathias S; Paananen, Arja; Szilvay, Géza R; Linder, Markus B. Dynamics and interactions of hydrophobin HFBII assembly in solution by stopped-flow spectroscopy. Submitted manuscript in the year 2015.

Author's Contribution

I. The author carried out all the experiments, planned the work, interpreted the results and wrote the publication in collaboration with the co-authors.

II. The author carried out QCM-D measurements including BCA assays and SAM surface preparation, performed Langmuir-through film preparation and surface pressure experiments, studies on plateau forming time, as well as part of the SEC studies and assisted in AFM measurements. The author planned the work and interpreted the results in collaborations with the co-authors and contributed to the writing of segments related to QCM-D and plateau forming time in the publication.

III. The author carried out all experiments except AFM measurements, planned the work, interpreted the results and wrote the publication in collaboration with the co-authors.

IV. The author carried out all the experiments, planned the work, interpreted the results and wrote the publication in collaboration with the co-authors.

1. Introduction

This work describes the properties of a group of proteins termed hydrophobins, which fulfil a variety of functions in the growth and function of filamentous fungi. The common button mushroom *Agaricus bisporus*, a common part of our normal diet, is an example of such a fungus expressing the protein. Hydrophobins function as coatings/protective agents, in adhesion, surface modification and overall functions that require surfactant-like properties (Wösten 2001; Linder et al. 2005). This thesis is concentrated on the hydrophobins HFBI, HFBII and HFBIII expressed by *Trichoderma reesei*.

Hydrophobins are small, about 10 kDa sized proteins that are surface active, meaning that they adsorb at the air-water interface lowering the surface tension of water. Comparing the properties and sequences of hydrophobins a classification of the proteins was made (Wessels 1994), where two classes where distinguished. The classes, class I and class II hydrophobins, were based on the occurrence of hydrophilic and hydrophobic amino acid residues in the protein sequence i.e. their hydrophaty plots (Kyte & Doolittle 1982). Class I hydrophobins form assemblies that appear to be more resistant towards solvents and detergents compared to class II hydrophobins and are highly insoluble in aqueous solution. Members of class II hydrophobins form assemblies that are much easier to dissolve. Furthermore, class I hydrophobins tend to form a mosaic of rod-like structures, called rodlets, on surfaces whereas class II hydrophobins do not. So far, class II hydrophobins have been found only in fungal taxonomic group of Ascomycetes, whereas class I hydrophobins have been found in both Ascomycetes and Basidiomycetes (Linder et al. 2005; Whiteford & Spanu 2002).

1.1 Biological functions of hydrophobins

Hydrophobins are involved in the adaptation of the fungi to the environment by altering interfacial interactions. Fungi have evolved to use hydrophobins for multiple tasks and most fungal genomes contain multiple copies of hydrophobins that may have different expression profiles. Fungal hyphae growing in aqueous medium secrete hydrophobins into the surrounding medium which adsorb at the air-water interface, lowering the water surface tension thereby enabling the hyphae to penetrate the air-water barrier and grow into the air (Wösten et al. 1999).

Hyphae growing into the air are also expressing hydrophobin genes and as the hydrophobins are not diffusing into a medium, they self-assemble between the hydrophilic cell wall and the air (Wösten et al. 1993; Wösten et al. 1994). As a result, aerial hyphae (Wösten et al. 1993; Wösten et al. 1994; Askolin et al. 2005), fruiting bodies (Wessels et al. 1991; Lugones et al. 1996; De Groot et al. 1997) and spores (Bell-Pedersen et al. 1992; Stringer et al. 1991) become hydrophobic. The hydrophobicity of aerial hyphae and fruiting bodies have been suggested as preventing the structures to fall back into the moist substrate (Wösten et al. 1993; Wösten et al. 1994), as well as to serve as a protection against bacterial and fungal infections (Wösten 2001). As much as 60 % of the total mRNA of the outer peel tissues of the caps of the common button mushroom *A. bisporus* is produced by the gene encoding the hydrophobin ABHI (HYPHA) (De Groot et al. 1997). Hydrophobins have also been shown to line gas channels of fruiting bodies thereby preventing the channels from filling with water (Lugones et al. 1999; van Wetter et al. 2000).

1.2 Hydrophobin role in nature

Fungi are important in the carbon cycle in their environment, in ecology, as well as being industrially and economically important. Fungi are used as biocontrol agents, for food- and enzyme production and e.g. for breaking down cellulose for biofuels and have a crucial role in nature in the breakdown and turnover of plant material. Fungi can also function as pathogens and cause damage on buildings and crops.

The amounts of hydrophobins secreted into the soil during breakdown and turnover of plant material by fungi are so high that geological effects such as changes in soil hydrophobicity are anticipated (Rillig 2005; Rillig et al. 2007). The soil might itself turn hydrophobic and water repellent as hydrophobins are resistant to degradation and have been shown to turn hydrophilic surfaces hydrophobic (Linder et al. 2005).

Hydrophobins have been shown to enable the attachment of hyphae to solid substrates including hydrophobic surfaces (Wösten et al. 1994; Talbot et al. 1996; Lugones et al. 2004). The hydrophobicity of spores has been suggested as facilitating the spreading in the environment by wind and insects as well as to prevent desiccation (Stringer et al. 1991; Bell-Pedersen et al. 1992; Temple et al. 1997). Hydrophobic fungal conidiospores with a hydrophobin coating can easily adhere to hydrophobic biotic or abiotic surfaces. Adsorption of pathogenic fungi to the surface of a host organism has also been shown to be involving hydrophobins (St Leger et al. 1992; Talbot et al. 1996; Kazmierczak et al. 2005). The hydrophobin gene mpg1 has been shown to be involved in the adhesion of the rice pathogen *Magnaporthe grisea* to its host (Talbot et al. 1996; Talbot et al. 1993) and expression of hydrophobins has also been shown for the tomato pathogen *Cladosporium fulvum* (Spanu 1997) suggesting that hydrophobins are widely important in the infection process of pathogenic fungi (Zampieri et al. 2010).

Hydrophobins also have roles in interactions between fungi and plants (Viterbo & Chet 2006), and have been shown to be important in the symbiotic interactions between fungi and plants, mycorrhizas (Tagu et al. 2001; Tagu et al. 1996; Mankel et al. 2002), as well as symbiotic interactions between fungi and algae or cyanobacteria, i.e. lichens (Scherrer et al. 2000).

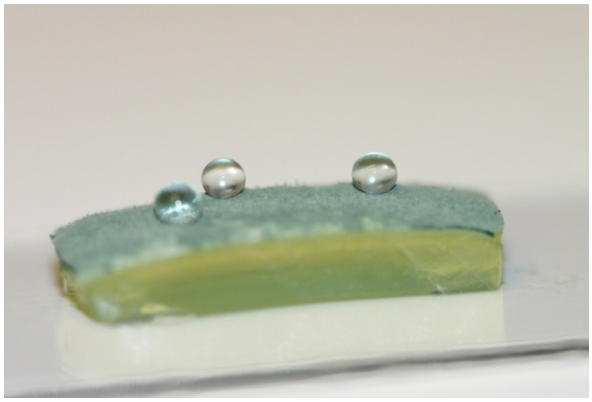

Figure 1. The surface of a mycelial mat of *T. reesei* growing on agar is highly hydrophobic as shown by water drop contact angles of about 140° (I)

1.2.1 Hydrophobin role in Immune recognition of spores

Hydrophobins have been shown to prevent immune recognition of airborne fungal spores, conidiospores (Aimanianda et al. 2009), and hiding the spores from clearance by neutrophils and macrophages in early stages of infection (Aimanianda et al. 2009; Paris et al. 2003; Shibuya et al. 1999; Bruns et al. 2010).

1.3 Structure of hydrophobins

The sequences of the two classes of hydrophobins share a unifying feature, where there are typically eight cysteine residues in a specific pattern. The second and third Cys-residues follow each other in immediate proximity, forming a pair, and a similar pair is formed by Cys-residues six and seven. The rest of the eight residues do not form pairs, resulting in a pattern of separated, pair, separated, separated, pair, separated (Linder et al. 2005; Wösten 2001).

1.3.1 Class II hydrophobins

The crystallographic structures of the class II hydrophobins HFBI and HFBII reveal important information on how hydrophobins function. The structure consists of a small antiparallel β-barrel formed by two β-hairpins connected by a stretch of α-helix (Figure 2). Proteins are often stabilized by hydrophobic interactions, but in these proteins the core is stabilized by an extended network of disulphide bonds. In hydrophobins, about 80 % of the hydrophobic side-chains are exposed on one side of the protein, forming a “hydrophobic

patch", a planar surface area formed by hydrophobic aliphatic amino acids, and formed to a large extent by two loop regions in the central β-barrel structure. In HFBII, the patch constitutes 12 % of the total surface area, which is otherwise mainly hydrophilic. The structure can thus be regarded as a protein amphiphile – a protein with distinct hydrophilic and hydrophobic regions. The hydrophobic patch can be seen comparing HFBI and HFBII to other class II hydrophobins, indicating an important functional role and suggesting a similar amphiphilic protein surface of all class II hydrophobins.

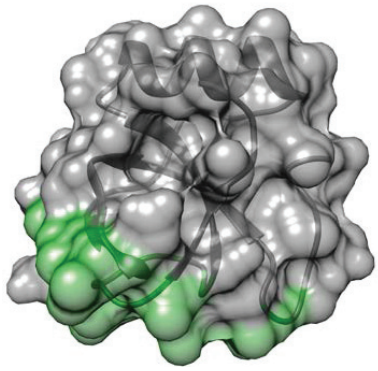

Figure 2. X-ray crystal structure of HFBII (PDB ID 2PL6) (Kallio et al. 2007) Cartoon of the surface representation of HFBII with the hydrophobic patch shown in green. The protein backbone visible showing a β-barrel formed by two β-hairpins and a connecting α-helix.

1.3.2 Class I hydrophobins

The structure of class I hydrophobins have been shown to be similar to structures of class II hydrophobins. The class I hydrophobins EAS from *Neurospora crassa* and SC3 of *Schizophyllum commune* shows a similar fold to HFBII (Kwan et al. 2006; Fan et al. 2006). Comparing EAS with HFBII it can be seen that the disulphide bridging pattern is the same as in HFBII. Differences can be seen comparing the hydrophobic patches of the proteins where much larger loops are formed between the strands of the beta barrel structure of EAS compared to HFBII.

1.4 HFB solution behaviour

The amphiphilic structure of hydrophobins is important for their function in aqueous solutions. Water molecules interact poorly with hydrophobic molecules, called the hydrophobic effect, and as a result hydrophobic molecules such as hydrophobins with their hydrophobic patch are clustered together, shielding the patches from water. In solution hydrophobins have been shown to form different dimers and oligomers. The class I hydrophobin SC3 has been shown to exist as monomers, dimers and tetramers in solution (Wang et al. 2004), whereas EAS has been suggested to occur only as monomers (Mackay et al. 2001). Class II hydrophobins HFBI and HFBII have been shown to form dimers and tetramers in solution (Torkkeli et al. 2002; Kisko et al. 2008),

clustered together through their hydrophobic patches (Hakanpää et al. 2004; Hakanpää 2006). Furthermore, oligomerization of HFBI has been shown to be dependent on hydrophobin concentration, as a change from monomers to tetramers was seen when the HFBI concentration increased. The HFBI multimers were shown to continuously disassemble and reassemble in solution. The affinity of solution multimerization of HFBI multimers was showed to be lower than the air-water interface affinity, and as a result hydrophobin was shown to adsorb at interfaces even in the presence of multimers (Szilvay et al. 2006; Szilvay, Kisko, et al. 2007). A continuous dynamic state between interface assembled hydrophobin and hydrophobin in solution has also been suggested by (Krivosheeva et al. 2013).

1.5 Interfacial self-assembly

The multimers formed in solution disassociate at interfaces and the hydrophobins rearrange and form surface membranes (Fan et al. 2006; Kallio et al. 2007; Wang et al. 2004; Szilvay, Paananen, et al. 2007). At the air-water interface hydrophobins assemble into films that can display a very ordered structure (Linder 2009; Szilvay, Paananen, et al. 2007). Class I hydrophobins form rod-like structures, called rodlets, about 5 -10 nm in width and several hundred nm in length, and can typically be seen when a solution of hydrophobin is dried down on a solid surface (Wösten et al. 1993). Class II hydrophobins have not been observed to form rodlets. Instead, e.g. HFBI, HFBII and HFBII have been shown to form interfacial films with a self-assembled hexagonally ordered structure (Figure 3) (Paananen et al. 2003; Kisko et al. 2005; Kisko et al. 2007). It has been shown that also multimers disassemble at the interfaces to form monolayers (Szilvay, Paananen, et al. 2007). The surface adsorbed films of class II hydrophobins are more easily dissolved than class I films.

Values of surface tension of hydrophobin films have been reported as high as 45 – 27 mNm^{-1} (Askolin et al. 2006; Lumsdon et al. 2005) and surface elasticity between 0.5 – 1.0 Nm^{-1} which is orders of magnitude higher than measured for any other surface active protein (Cox et al. 2007, II). The high surface elasticity of hydrophobins is connected to their tendency to form very stable foams (Bailey et al. 2002; Sarlin et al. 2005). Foams and bubbles of HFBII have been shown to be stable for months and even years (Cox et al. 2009).

Hydrophobins have been shown to efficiently adhere to surfaces. Adhesion onto hydrophobic surfaces has been studied extensively (Lugones et al. 1996; Wang et al. 2010; Askolin et al. 2006; de Vries et al. 1999; De Stefano et al. 2008). E.g. SC3 has been shown to be able to bind to Teflon and form a very insoluble layer (de Vocht et al. 2002). The assembly of class II hydrophobins onto polar hydrophilic surfaces under aqueous solution is studied in Publication III. Previously, coating on hydrophilic surfaces has been performed by drying down a hydrophobin film typically on filter paper were the film was first formed at the air-water interface (Wösten & de Vocht 2000). Class I hydrophobin HGFI has been shown to slightly increase the hydrophobicity of a hydrophilic mica surface (Hou et al. 2009).When binding to solid surfaces,

hydrophobins can form films that are very tightly bound, with class I generally adhering more strongly than class II hydrophobins (Askolin et al. 2006). Interestingly, Class I and class II hydrophobins have also been shown to form mixed membranes despite their differences in adhesion strength.

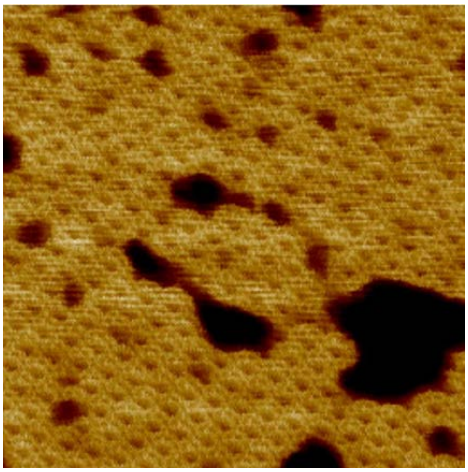

Figure 3. HFBI self-assembled at the air-water interface into a hexagonally ordered monolayer. Imaged with tapping mode in air on mica, image size 100 nm x 100 nm (Image courtesy of Arja Paananen)

1.5.1 Recruitment of molecules to surfaces

Hydrophobins of both classes are able to adsorb proteins and molecules when bound to a surface without losing activity. Glucose oxidase (GOx) of *Aspergillus niger,* bovine serum albumin (BSA), chicken egg avidin and monoclonal IgG has been shown to adsorb onto a solid hydrophobic surface coated with Class I hydrophobin HGFI or class II hydrophobin HFBI (Wang et al. 2010; Qin et al. 2007). The adsorption of these proteins was suggested as being dependant on electrostatic interactions, and the hydrophobins were shown to transform a non-polar surface into a polar one and to adsorb proteins specifically without denaturation of the adsorbed proteins (Wang et al. 2010; Qin et al. 2007). Hydrophobins adsorbed on surfaces have been used to immobilize enzymes (Zampieri et al. 2010; Palomo et al. 2003). E.g. a film of adsorbed hydrophobin RolA was shown to specifically recruit the enzyme CutL1 to the surface (Takahashi et al. 2005). The immobilization of enzymes has also been suggested as possible uses in biosensors (Corvis et al. 2006; Zhao et al. 2009; Hou et al. 2009; Bilewicz et al. 2001), e.g. the class I hydrophobin SC3 has been used to immobilise GOx and horseradish peroxidase (HRP) onto glassy carbon electrodes (Corvis et al. 2005).

1.6 Application potential of hydrophobins

Application potential for hydrophobins has been suggested for both technical and medical applications. Biocompatible surfaces are needed for various bio-

medical applications such as implants and artificial tissues, and hydrophobin coatings have been suggested to increase the biocompatibility by preventing immunogenic reactions, as hydrophobin coating in spores has been shown to prevent immune recognition of airborne fungal spores (Aimanianda et al. 2009; Zampieri et al. 2010). Hydrophobin coated polystyrene has showed promising results in terms of biocompatibility (Misra et al. 2006). Also cell growth on Teflon (Janssen et al. 2002; Scholtmeijer et al. 2002) and poly(dimethylsiloxane) (PDMS) (Hou et al. 2008) using hydrophobins has been shown.

In order to selectively create films, engineered hydrophobins can function as adsorption mediating modules conjugated with DNA-binding macromolecules, (Kostiainen et al. 2006), chelating groups (Corvis et al. 2006) as well as fused with enzymes (Linder et al. 2002) or protein binding targets (Szilvay, Paananen, et al. 2007). An engineered version of class I hydrophobin DewA has been used to deposit a thin film of titanium dioxide on top of a self-assembled layer of the hydrophobin. Silicone surfaces and graphene have been functionalized with gold nanoparticles using HFBI derivatives (Laaksonen et al. 2009; Laaksonen et al. 2010). Films based hydrophobins could be included in biosensors, diagnostic kits, photonic devices and microelectronics (Linder 2009). Hydrophobins have e.g. been shown to form a KOH protective coating on a silicon surface, demonstrating the use of hydrophobins during etching for silicon micromachining techniques (De Stefano et al. 2007).

Hydrophobins can also be used to stabilize hydrophobic liquids in water such as emulsions for cream or ointments for pharmaceutical or cosmetic use. The ability to easily form stable foams (Bailey et al. 2002; Cox et al. 2009) can be used to produce foams for food products and to detect foaming agents where excessive foaming is unwanted, e.g. beer (Sarlin et al. 2005).

Hydrophobins have also been suggested as a method to make drugs accessible for oral (Haas Jimoh Akanbi et al. 2010), topical (Vejnovic et al. 2010) or intravenous (Fang et al. 2014) delivery. Furthermore, coating on drug-loaded nanoparticles for possible drug delivery has been studied (Valo et al. 2010; Sarparanta et al. 2012)

Aims of the study

Related to the remarkable properties of hydrophobins, a largely unanswered question is in what manner hydrophobins function when interacting with their surroundings and how their surroundings affect their function. Following this, the aim of this study is to examine the following issues:

1. How do hydrophobins function when interacting with their surroundings?

2. How do proteins, molecules and interfaces surrounding hydrophobins interact with hydrophobins and thereby affect their function?

These issues are in this work examined by studying how hydrophobins function when assembling on different types of surfaces including nanoparticles, how they function when interacting with their surroundings to recruit other proteins and molecules, and how their structure is affecting their self-assembly and recruiting behaviour. The effect of different surfaces on hydrophobin self-assembling function, and how hydrophobins behave in terms of solution dynamics and how surrounding proteins and molecules affect this behaviour is also examined.

2. Materials and Methods

A summary of the materials and methods used in this study is presented in this section. More detailed information is given in the publications I – IV.

2.1 Hydrophobins

The class II hydrophobins HFBI, HFBII and HFBII were purified from either mycelium or culture supernatant of *T. reesei* using two-phase extraction and reversed phase chromatography (Paananen et al. 2003; Linder et al. 2001). FRET variants are described in (IV), variants of charged residues in (II).

2.2 Surface characterization methods

2.2.1 Quartz crystal microbalance with dissipation

In quartz crystal microbalance with dissipation (QCM-D), resonance frequency and dissipation is measured simultaneously and the mass of a bound protein layer can be calculated using the Sauerbrey relation, $\Delta m = -C\Delta f/n$, where Δm is adsorbed mass, Δf is frequency change, C = 17.7 ng Hz cm−2, and using the third overtone (n = 3) (D4-QCM system, Q-Sense, Sweden). By combining the frequency measurements with dissipation measurements, the rigidity of the formed layer can be determined depending on decay of oscillations of the layer thereby describing the viscoelastic properties of the layer. Hydrophobins were dissolved in buffer at 0.1 mg/mL and protein solution (300 µL) was pumped through the measuring chamber with a flow rate of 100 µL/min. The sensors were left to stabilize until a stable signal was achieved and then washed with running buffer (II, III).

2.2.2 Water contact angle

Water contact angle (WCA) is a measure of surface hydrophobicity. A drop of typically 6 µL Milli-Q water was applied on a surface and the average contact angle of the drop on the surface is calculated from a series of 15 pictures with a 5 s interval, as an average of three measurements (CAM 200, KSV NIMA, Finland). Here, WCA values were measured before and after hydrophobin adsorption (III).

2.2.3 Atomic force microscopy

Atomic force microscopy (AFM) was used for imaging of LB-films formed on mica using a NanoScopeV Multimode 8 AFM (E scanner, Bruker, Germany). A scanning probe image processor (SPIP, Image Metrology, Denmark) was used for image analysis. Topography images were acquired using tapping mode in air using scan rates in the range of 0.7 - 1 Hz where amplitude changes in oscillations of a cantilever driven by a small piezoelectric element is detected in order to gain information of surface topography and phase contrast (Geisse 2009). Topography and phase contrast images were captured simultaneously. (II)

2.2.4 Langmuir film preparations

Langmuir Blodgett (LB) through was used to compress surface layers of hydrophobin at the air-water interface in a controller manner in order to measure surface pressure and produce monolayers on mica for AFM measurements.

Surface pressure of a hydrophobin monolayer was analysed in a humidified atmosphere using a Langmuir through and pre-soaked 20.6 mm perimeter Wilhelmy paper plates (KSV Minimacro Trough, KSV NIMA, Finland). The hydrophobin sample was dissolved at a concentration of 0.85 – 1.0 μM by short magnetic stirring prior to probing. Surface pressure was measured at equilibrium (typically reached after 20 min – 1 h) The Wilhelmy plate was submerged prior to protein addition.

LB films: A monolayer of hydrophobin was assembled by injecting 20 μg of dissolved protein into 55 mL of 5 mM Na-acetate buffer pH 5.5 at 21° C. After the surface pressure had been stabilized (typically 45 minutes) the compression of the protein monolayer formed at the interface was started and compressed at a barrier speed of 2 mm/min until 35 mN/m surface pressure was reached. A monolayer of hydrophobin was then transferred to a flat mice substrate for AFM imaging (II).

2.3 Solution association analysis methods

2.3.1 Förster resonance energy transfer

Förster resonance energy transfer (FRET) is here used to measure the efficiency of energy transfer E, determined by measuring the enhanced fluorescence of an acceptor fluorophore in a fluorescence spectrophotometer (Cary Eclipse, Varian, USA). A donor fluorophore initially in its excited state transfers energy to an acceptor fluorophore when in close proximity. Here engineered variants of HFBII, HFBII-CysC were used which has an additional Cys residue at the C-terminus, conjugated with either cyanine dye 3 (donor) or cyanine dye 5 (acceptor) forming a FRET pair for measurements (Clegg 1992). Samples used here were excited at 516 nm (donor excitation) and the emission spectra from

both donor and accepter was recorded in order to determine hydrophobin multimerization states at different concentrations (IV).

2.3.2 Stopped-Flow spectroscopy

Stopped-Flow spectroscopy (SF) is used to study the kinetics of fast reactions in solution. Donor and acceptor are placed in two different syringes and liquid from both syringes are simultaneously injected into a small cuvette after which the flow is stopped and the resulting fluorescence is measured (Clegg 1992) (Chirascan SF.3 spectrometer, Applied Photophysics, UK). Here, the FRET pair of cy3 and cy5 labelled HFBII-CysC were used. A change in fluorescence could be seen as described regarding FRET, as a change in hydrophobin monomer association or disassociation occurring in the sample. Each syringe was loaded with 100 µg/ml hydrophobin, 10 µg/ml labelled and 90 µg/ml wild-type hydrophobin. The addition of wild-type was made in order to achieve appropriate fluorescence signal. The drive volume was set to 140 µL and FRET signal was measured at acceptor emission of 665 nm.

Activation energy, (Ea) was determined by measuring the exchange rate at three different temperatures, 21.5°, 17.5° and 12.5° Celsius in order to examine the temperature dependency of hydrophobin multimerization. The Arrhenius equation, k=Ae^(-Ea/RT)gives activation energy Ea and frequency factor A by plotting ln(k) vs. 1/T, where k is the reaction rate constant and T temperature (K). The reaction rate constant was here attained by using Pro-data viewer (Applied Photophysics, UK) using a Marquardt-Levenberg algorithm. The algorithm iterate until convergence to a chosen suitable equation, here a single exponential, a*e(-kx) +c where k is the reaction rate constant. The time needed for half of the hydrophobin multimers in solution to exchange is described as $t_{1/2}$ and was calculated as ln(2)/k (IV).

2.3.3 Size exclusion chromatography

Size exclusion chromatography (SEC) was used in order to examine concentration dependency of hydrophobin multimerization. Superdex 75 column and Äkta explorer (GE, USA) was used (II, IV).

2.4 Size measurements

2.4.1 Differential centrifugal sedimentation

Differential centrifugal sedimentation, DCS measures particle size distribution using centrifugal sedimentation within an optically clear spinning disc filled with fluid and here determines nanoparticle size on a nanometre level based on the sedimentation time of a particle through a glucose gradient (CPC disc centrifuge DC24000, CPS Instruments, USA). DCS measures apparent diameter size which makes it necessary to correct for changes in density of e.g. adsorbed protein layers on a nanoparticle by a core shell model in order to attain accurate size determination of protein shell coated nanoparticles. DSC meas-

urements are calibrated in order to apply the core-shell model $\frac{(\rho_c - \rho_s)}{(\rho_c - \rho_f)}\frac{D_c^3}{D_s} + \frac{(\rho_s - \rho_f)}{(\rho_c - \rho_f)}D_s^2 = D^2$, where ρ_c and D_c describes density and diameter of a core particle with a shell of density ρ_s and thickness D_s placed in a rotating disc filled with a fluid of density ρ_f giving the measured diameter D. (I, (Monopoli et al. 2011)

2.4.2 Dynamic light scattering and zeta potential

Dynamic light scattering (DLS) and zeta potential measures size and surface charge in terms of zeta potential, here on nanoparticle and protein dispersions (Zetasizer ZS, Malvern ,UK). Data is reported as average hydrodynamic diameter and a measure of size distribution. Polydispersity, PDI, is also given as a measure of aggregation (II, III).

2.5 Other

2.5.1 Self-assembled monolayers

Self-assembled monolayers (SAMs) are here created by dissolving cleaned gold disks overnight in a solution of long-chained molecules with a head group for anchoring, a tail and a functional end group dissolved in ethanol which self-assemble to attain ordered surfaces (Ulman 1996), here cationic, anionic and nonpolar aliphatic surfaces used for QCM-D measurements. For cationic surfaces N,N,N-trimethyl-(11mercaptoundecyl)ammonium chloride (HS(CH2)11NMe3+Cl–) thiol (TMA) (Prochimia Surfaces, Poland) was used. For hydrophobic surfaces 1-hexanethiol (HEX) (Sigma-Aldrich, USA) was used, and for anionic surfaces 1-mercaptoundecanoic acid (MUA) (Sigma-Aldrich) was used. SAMs were coated on either QCM-D sensor disks (QSX 303, Q-sense, Sweden) or gold coated glass disk (Bionavis, Finland) (II, III)

2.5.2 Dialysis

Dialysis is a method to remove material from a solution, here used in order to remove free or loosely bound hydrophobin from nanoparticles by diffusion through a semipermeable membrane (Float-A-lyzer G2, 1 ml 50 kDa, Spectrum Labs, USA). A sample of nanoparticles and hydrophobin was loaded into the dialysis device floating in 1 L buffer (PBS pH 7.4) at 4° under continuous stirring, after changing to fresh buffer every day the buffer was changed to MQ water in order to avoid aggregation of particles (I).

2.5.3 SDS-PAGE

SDS-PAGE is used to separate proteins based on their size. Polyacrylamide gel electrophoresis (PAGE) using sodium dodecyl sulphate (SDS) which linearizes protein and imparts an even negative charge per unit mass enabling separa-

tion based on size (Shapiro et al. 1967). 4 % stacking gel and 15 % or 8 % resolving gel was used here in order to separate proteins recovered from nanoparticle surfaces (I).

3. Results and discussion

This work initially focuses on hydrophobin assembly onto nanoparticles and the subsequent recruitment of plasma proteins in order to describe the self-assembly and recruiting properties of the hydrophobin proteins (I). In order to further describe hydrophobin interaction with its surrounding, the abilities to form surface films on varying surfaces and interfaces by self-assembly and to selectively recruit proteins to surface films are examined. In order to study the roles and function of charged side chains of the protein, point mutations of the residues on HFBI were produced (II). Following this, the role of the hydrophilic side of hydrophobins replicating anchoring of the proteins on spores and cell walls and thereby rendering them hydrophobic are described as well as the roles of charged residues on the hydrophilic side in terms of interactions with polar surfaces by allowing hydrophobins to assemble onto solid polar hydrophilic surfaces in solution (III). Lastly, hydrophobin solution dynamics is described in terms of hydrophobin solution multimer exchange and how the exchange is affected by the environment on terms of other hydrophobins, proteins and surfactants (IV).

3.1 Hydrophobin self-assembly on surfaces and recruiting of proteins (I)

All hydrophobins adhere to surfaces, and hydrophobins have been shown to play important roles as coatings of fungal spores (Wösten 2001; Linder et al. 2005). Hydrophobin HFBII was allowed to physically adsorb on monodisperse carboxylated (PCOOH) and sulfonated ($PSOSO_3$) polystyrene nanoparticles (NPs) of nominally 100 nm and 200 nm in diameter. The sulfonated NPs can be seen as more hydrophobic. HFBII binding onto NPs was examined with Dynamic light scattering (DLS), Differential centrifugal sedimentation (DCS) and SDS-PAGE and protein binding was seen on both types of particles (I). In order to examine the ability of hydrophobins to recruit other proteins to surfaces, human plasma proteins were allowed to adsorb on the NP-HFB complexes (I).

3.1.1 Form layers on NP surface by self-assembly

HFBII binding to NPs was examined using DLS, DCS and SDS-PAGE. NP size and charge were examined on both pristine (uncoated) particles and on NPs after incubation with HFBII. Hydrophobin coating was done using a dialysis process. Figure 4 shows how HFBII was successfully adsorbed on the two types of NPs of both sizes, seen as a strong and consistent band of 7 kDa.

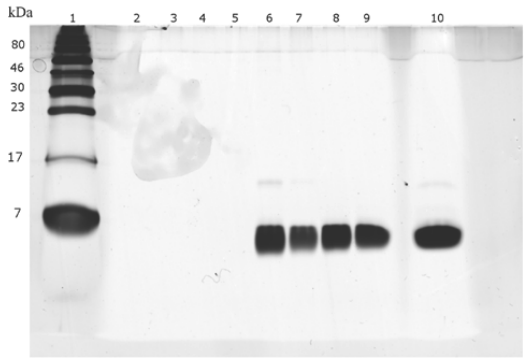

Figure 4. SDS-PAGE gel showing the adsorption of HFBII to 100 and 200 nm carboxylated and sulfonated NPs. Lane 1: ladder; lane 2: 100 nm carboxylated NP; lane 3: 200 nm carboxylated NP; lane 4: 100 nm sulfonated NP; lane 5: 200 nm sulfonated NP; lane 6: 100 nm carboxylated NP with HFBII; lane 7: 200 nm carboxylated NP with HFBII; 8: 100 nm sulfonated NP with HFBII; 9: 200 nm sulfonated NP with HFBII; 10: HFBII control sample.

In DCS measurements, protein adsorption and NP size was measured as a change in density where particle apparent size seen as a change of sedimentation time. A core shell model was applied for accurate size measurement of protein layer thickness using the known density of the protein (I). NPs of 200 nm in size are shown as an example in Figure 5. The results show that NPs of both types and sizes resulted in a shift in apparent size (Table 1) as a result of change of density and/or protein binding. A stronger and more severe shift was observed with sulfonated NPs suggesting stronger binding.

The shell thickness for the 200nm NPs was calculated as 2.3 nm and 1.4 nm for sulfonated and carboxylated respectively (Figure 5). On the sulfonated NPs, a layer of dimensions similar to a theoretical monolayer was thus seen, as the he approximate diameter of a single hydrophobin is about 2 nm. For 100 nm NPs, the shell thickness was calculated to be 1.2 and 0.3 nm for 100 nm sulfonated and carboxylated NPs respectively. This data suggests a more uniform protein layer being formed on sulfonated particles. Looking at approximated diameters on DLS measurements, where a change of hydrodynamic radius is larger on sulfonated NPs, and at 100 carboxylated NPs relatively unchanged, supporting the theory of lower protein binding and less uniform layers being formed on these particles (Table 2).

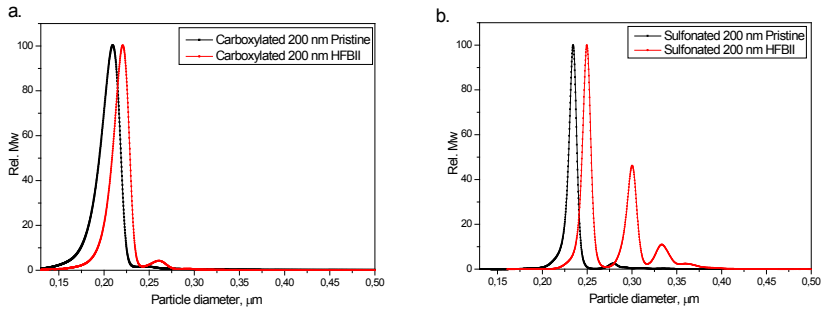

Figure 5. DCS experiments of 200nm carboxylated (a) and sulfonated (b) PS NPs on pristine NPs and on NP- HFBII complexes.

Sample		**Particle apparent size (by DCS)**		**Shell thickness nm**
Surface modification	Particle nominal size [nm]	Pristine [nm]	NP-HFB [nm]	
carboxylated	100	113.2	116.3	0.3
	200	209.6	221.1	1.4
sulfonated	100	96.6	106.1	1.2
	200	234.3	251.4	2.3

Table 1. NP-HFBII: Shell thickness by DCS

The surface charge in terms of zeta potential of NP-HFBII complexes compared to pristine NPs showed similar values in both cases looking at carboxylated NPs. However, the zeta potential of sulfonated NPs was reduced from about 50 mV on pristine NPs to about 30 mV on NP-HFBII complexes of both sizes. This further suggests a more uniform layer being formed on the sulfonated particles, as a thicker layer also was seen in DCS and DLS experiments on these particles. Furthermore, these results also imply that the charged side chains on the hydrophilic side of HFBII can possibly interact and form different type of layers on the two NPs. Hydrophobin HFBI bind differently in terms of orientation on surfaces with varying polarity as is shown in publication III and these differences on surface charge on NP-HFBII complexes suggests that this could be the case also on for HFBII on NPs.

Sample			DLS				
Surface modification	Particle size [nm]	Sample coating	Dm, [nm]	SD	PDI	Zpot [mV]	SD
carboxylated	100	Pristine	111.4	0.6	0.03	-46	0.8
		NP-HFB	111.0	1.7	0.02	-47	1.6
	200	Pristine	196.1	0.8	0.02	-50	1.0
		NP-HFB	202.3	1.9	0.01	-44	0.5
sulfonated	100	Pristine	103.2	0.8	0.04	-50	3.1
		NP-HFB	120.6	1.2	0.09	-28	0.6
	200	Pristine	234.5	1	0.02	-47	0.6
		NP-HFB	302.5	1.4	0.21	-32	1.7

Table 2. NP-HFBII: Z-potential, size by DLS

3.1.2 Recruitment of plasma proteins

In order to examine the recruitment of proteins to a surface via bound hydrophobins, human plasma was allowed to bind onto NP-HFB complexes. A few tens of about 4000 human plasma proteins form a strongly bound protein layer (corona) on NPs, called the hard corona (HC). An external layer of proteins with less affinity, the soft corona, is in exchange with the environment, whereas the HC proteins are in slow exchange. The HC is analysed after separating and washing. The corona of NPs directly in plasma, unwashed and unseparated, is called *in situ* corona (IS).

In HC measurements, the pristine sulfonated NPs generated strong aggregation in presence of plasma making size measurements in DCS difficult. On sulfonated NP-HFBII complexes, aggregation was small, allowing for protein size measurements (Figure 6). Looking at carboxylated NPs, HFBII is reducing the calculated corona thickness compared to pristine NPs (Table 3).

In IS measurements, sulfonated pristine NPs also generated aggregation, but apparent size was however measurable. As was seen in HC measurements, HFBII reduced aggregation dramatically. A hydrophobic coating on both sulfonated and carboxylated NPs of both sizes resulted in a considerate decrease in the corona thickness compared to the corona formed on pristine NPs (Table 3).

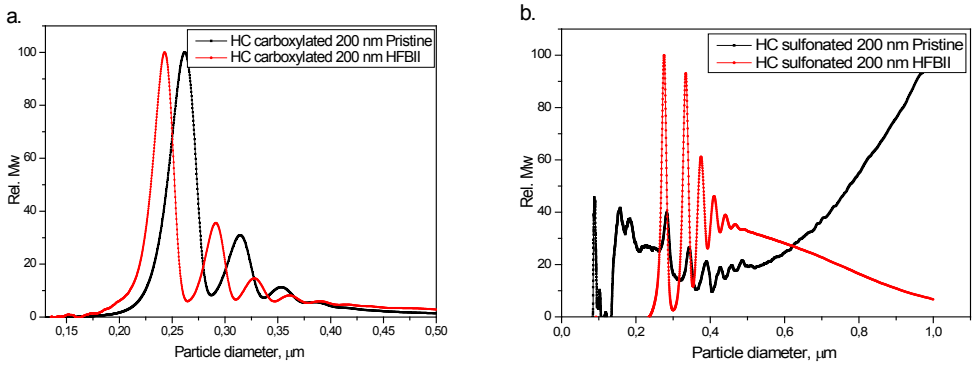

Figure 6. DCS of particles with HC. Performed on pristine NPs and NP – HFBII complexes. Here represented by 200 nm NPs.

Sample			IS			HC		
NP	Particle size [nm]	Sample coating	Plasma corona [nm]	Change [nm]	[%]	Plasma corona [nm]	Change [nm]	[%]
carboxylated	100	Pristine	7.5			6.4		
		NP-HFB	6.3	-1.2	-16	4.7	-1.7	-26.6
	200	Pristine	8.3			7.2		
		NP-HFB	3.7	-4.6	-55	3.1	-4.1	-56.9
sulfonated	100	Pristine	6.9			Agg.		
		NP-HFB	4.5	-2.4	-35	1.6		
	200	Pristine	11			Agg.		
		NP-HFB	6.2	-4.8	-44	3.3		

Table 3. NP Protein Corona thickness by DCS.

In order to examine the HC plasma protein composition, plasma proteins were removed from the particles by reducing and heating in SDS and separated by SDS-PAGE, 15 % and 8 % (Figure 7). SDS-PAGE of IS plasma proteins was not carried out as the result would be inconclusive since non-bound plasma would be seen in the staining. In HC, SDS-PAGE indicated that plasma proteins adsorb on NPs in all cases. All HFBII treated NPs show a clear HFBII band at 7 kDa in the 15 % gel, a band that was missing on all NPs not in contact with hydrophobin. It is noteworthy that HFBII remained strongly associated to all NPs also after incubation in a competitive environment of plasma proteins. In order to look at the HC plasma protein layer composition, an 8 % SDS-PAGE gel was run where proteins of 250-60 kDa have better resolution. Interestingly, the levels of several HC plasma proteins were affected comparing NP-HFBII complexes to pristine NPs, especially in the case of sulfonated particles. The amounts of smaller plasma proteins were altered in the presence of HFBII in all four cases of NPs and sizes. HFBII did thus seem to have not only an effect on the apparent size and calculated corona thickness but also on the composition of the corona.

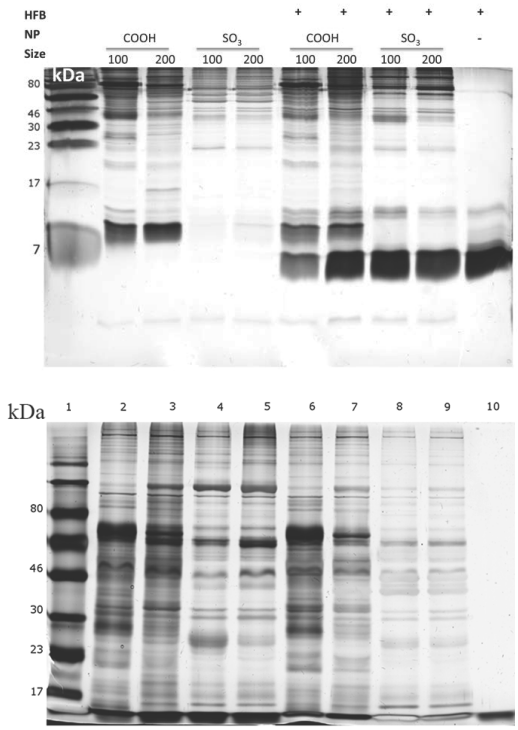

Figure 7. (top) 15 % SDS-PAGE of human plasma proteins free from excess plasma obtained from the hard corona of carboxylated (COOH) and sulfonated (SO_3) nanoparticles. Sample identification is provided on the top of the gel. (bottom) 8 % SDS-PAGE of human plasma proteins free from excess plasma obtained from the hard corona of carboxylated and sulfonated nanoparticles, 100 and 200 nm with pristine and covered with HFBII. Sample order:

1. Ladder, 2. carboxylated 100 nm +HFBII + Corona, 3. carboxylated 200 nm + HFBII + Corona, 4. Sulfonated 100 nm + HFBII + Corona, 5. Sulfonated 200 nm +HFBII + Corona, 6. carboxylated 100 nm + Corona, 7. carboxylated 200 nm + Corona, 8. Sulfonated 100 nm + Corona, 9. Sulfonated 200 nm + Corona, 10. HFBII

HFBII was here shown to strongly adsorb on polystyrene nanoparticles of varying polarity. A stronger binding was seen on the more hydrophobic sulfonated polystyrene NPs where a layer thickness of about a monolayer of 200 nm was observed. Hydrophobin HFBI bind differently in terms of orientation on surfaces with varying polarity as is shown in publication III and differences on surface charge on NP-HFBII complexes suggests that this could be the case also on NPs. The charged side chains on the hydrophilic side of HFBII can possibly interact and form different type of layers on the two nanoparticles.

HFBII was also shown to be tightly bound to the NPs also in competition with human plasma proteins. Adsorption of HFBII on the particles significantly reduced aggregation on sulfonated NPs in plasma suggesting use as an agent to increase bioavailability. Hydrophobins have previously been used to increase bioavailability of Teflon nanoparticles (Lumsdon et al. 2005), and have been suggested to improve dispersions of materials with advantageous electrochemical such as highly oriented pyrolytic graphite (HOPG), two-dimensional crystalline graphene, and single- and multi-walled carbon nanotubes (CNT) (Wösten & Scholtmeijer 2015).

On both types of NPs examined, hydrophobins showed a potential ability to recruit other proteins bound to a surface, as an adsorbed layer of hydrophobin was shown to bind a layer of plasma proteins forming a protein corona different in both composition and mass compared to plasma coronas formed on pristine NPs.

3.2 Interfacial assembly and interactions of other proteins, role of charged residues (II)

In order to further examine hydrophobin interaction with its surrounding, the ability of HFBI to form surface films on surfaces and interfaces by self-assembly and to selectively recruit proteins to surface films was studied. In order to examine the roles of charged side chains of the protein, point mutations of the residues on HFBI were produced (II).

3.2.1 Mutation variants of HFBI

HFBI possesses six charged residues that are exposed on the protein surface (Figure 8). Four of these are located on the face of the protein opposite of the hydrophobic patch (D40, D43, R45 and K50). The remaining two, D30 and K32, are located near the edge of the hydrophobic patch. Mutation variants were produced in four different types by neutralizing charged residues by replacing the charged residues with electrically neutral ones (II). The residues D30 and K32 located near the hydrophobic patch and potentially important for intermolecular interactions (Magarkar et al. 2014) were neutralized to form mutation D30N/D32Q. Neutralized positively charged residues formed the

negatively charged variant R45Q/K50Q, the positively charged variant D40Q/D43N was formed with neutralized negatively charged residues and a neutral variant with all charged residues neutralized was named D40Q/D43N/R45Q/K50Q.

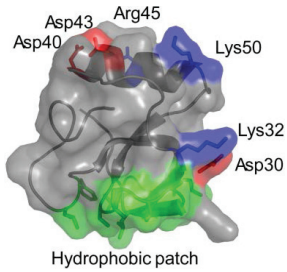

Figure 8. Three-dimensional structure of *T. reesei* hydrophobin HFBI (PDB-ID 2FZ6). Basic and acidic residues are annotated and coloured blue and red, respectively (II).

3.2.2 Behaviour of adhesion, effect of charged residues

HFBI variants and wild-type hydrophobin was allowed to bind onto hydrophobic 1-hexanethiol (HEX) self-assembled monolayer (SAM) surfaces. In order to measure protein adhesion and adsorption of the bound protein layer on the coated surfaces, QCM-D was used to detect frequency and dissipation and convert into bound mass (Figure 9, II). The adsorption into the hydrophobic surface was shown to be very similar among the tested HFBI variants and also in the range of adsorption of wild-type HFBI (Table 4).

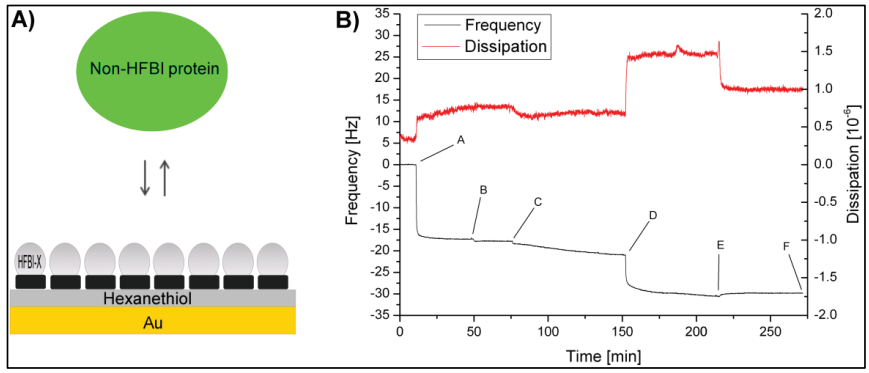

Figure 9. A) Schematic representation of the HFBI coated QCM sensor at which adsorption of non-HFBI proteins was measured; B) Representative protein adsorption QCM experiment at pH 9.0 with HFBI variant D40Q/D43N: (A) Injection of 0.03 mg HFBI-D40Q/D43N in 10 mM Na acetate buffer (pH 5.5), (B) removal of unbound hydrophobin by buffer rinsing, (C) equilibration with 10 mM glycine buffer (pH 9.0), (D) injection of 0.3 mg glucose oxidase at pH 9.0, (E) washing off of unbound glucose oxidase, (F) end of experiment. The adsorbed mass of the non-HFBI protein was calculated using the frequencies at points D and F.

	wild type	D30N/K32Q	D40Q/D43N	R45Q/K50Q	D40Q/D43N/R45Q/K50Q
HAM [ng/cm^2]	223 ± 98	247 ± 35	289 ± 45	217 ± 35	293 ± 56
γ [mN/m]	35.5 ± 1.6	36.5 ± 0.0	31.3 ± 7.5	36.0 ± 0.6	36.6 ± 0.3
t_{DF}	19 ± 3.5	24.3 ± 1.2	32.3 ± 2.5	23.7 ± 3.8	31.3 ± 3.5

Table 4. The hydrophobically adsorbed mass (HAM) was determined from the presented QCM experiments on hexanethiol coated surfaces. (γ) were determined from interfacial HFBI protein layers assembled in a Langmuir trough. (t_{DF}) represents time required for plateau formation of droplet of hydrophobin in solution, measured in triplicate.

3.2.3 Recruitment of other proteins to surfaces

The binding of proteins to self-assembled hydrophobin layers was examined with QCM-D. This was done by adding secreted *T. reesei* enzymes XYNI, XYNII, CBHI and EGII to adsorbed layers of HFBI, wild-type and variants, formed on hexanethiol-coated surfaces. As a reference, Glucose oxidase (GOx) of *A. niger* was in the same matter added to the hydrophobin layer.

GOx was found to interact strongly with the wild-type and all variants, with highest amounts bound at pH 4.7 – 5.7. A second adsorption maximum was measured for variant D40Q/D43N at pH 6-9 (Figure 10A).

No binding was detected with XYNI and EGII (Figure 10B, E). XYNII bound exclusively variant D40Q/D43N, with a binding maximum of 100 ng/cm^2 at around pH 5.2 and around 60 ng/cm^2 in other pHs measured (Figure 10C). In the case of CBHI, wild-type HFBI and variants R45Q/K50Q as well as D40Q/D43N bound between pH 3.9 – 4.7. D40Q/D43N binding of CBHI was considerably higher (570 ng/cm^2 at pH 4.7 than wild-type HFBI (60 ng/cm^2 at pH 3.9) and R45Q/K50Q (20 ng/cm^2 at pH 3.9)(Figure 10D).

Hydrophobins have previously been shown to form protein films and to bind other molecules to this film (Bilewicz et al. 2001; Corvis et al. 2006; Qin et al. 2007; Zhao et al. 2007; Palomo et al. 2003). Furthermore, it has previously been suggested that interactions between hydrophobin and a second layer of proteins are due to electrostatic interactions (Wang et al. 2010). In this work, binding of *T. reesei* enzymes XYNII and CBHI is shown to be very selective in terms of charged residues in HFBI surface. HFBII adsorbed on NPs was shown to adsorb layers of human plasma proteins in different manner when adsorbed on NPs of varying polarity, supporting the conclusion of importance of charged residues (I). Adsorption of hydrophobins on two structurally different anionic surfaces generated very similar results in term so binding and hydrophobicity of bound layer, which compared to a very low binding on anionic surfaces, indicates that specific charge is very important (III). However, hydrophobins might be able to assemble on surfaces in defined orientations related to each other, and to form pores and pockets with structurally defined environments (Figure 11) according to computational modelling. Such pockets can form very selective environments, as has been shown using cyclodextrins (Ling et al. 2008). The structure on the hydrophobin layer can thus have a large effect on the adsorption selectivity. Detailed conclusions on the nature of interactions between hydrophobin layers and a secondary layer of molecules cannot be drawn, but the binding of a secondary layer however seems to be very specific.

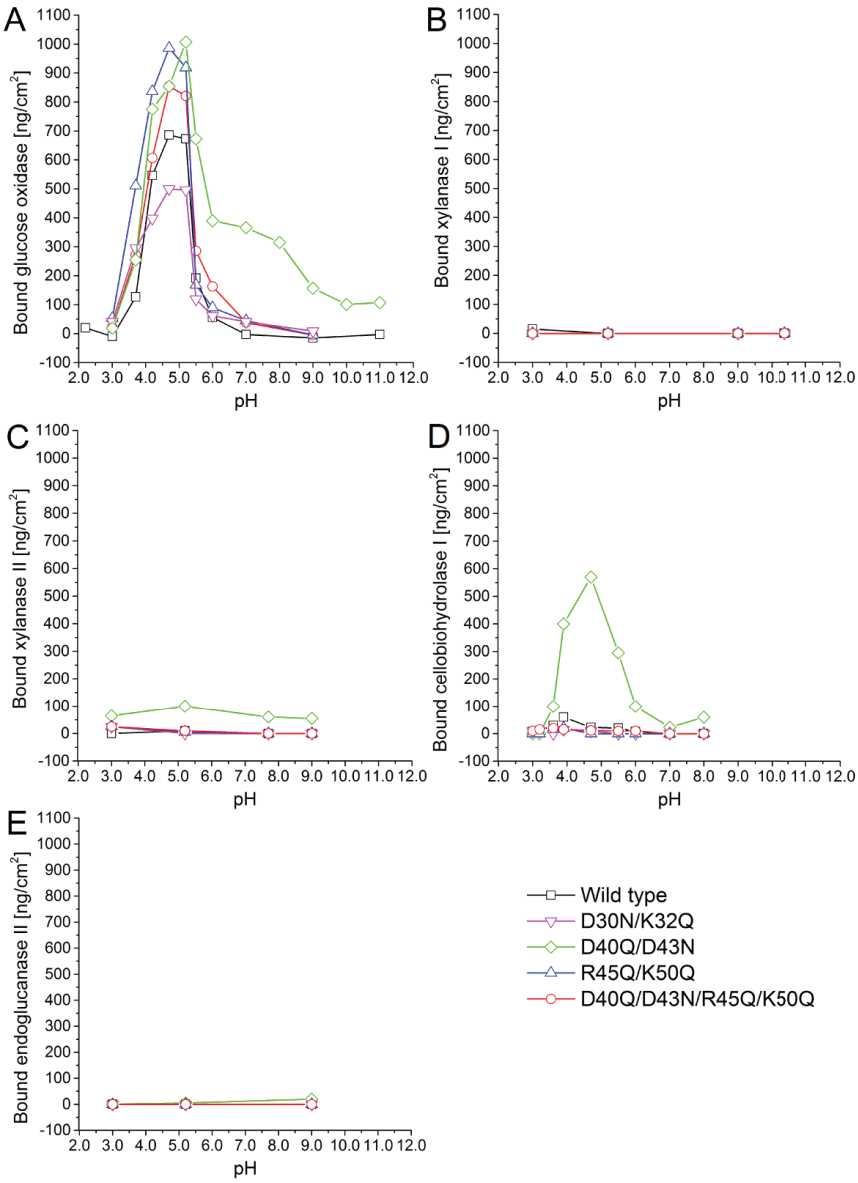

Figure 10. pH-Dependent adsorption of non-HFBI proteins to adsorbed layers of HFBI wild type and HFBI variants D30N/K32Q, D40Q/D34N, D40Q/D34N/R45Q/K50Q and R45Q/K50Q determined by QCM-D. The injected non-HFBI proteins were *Aspergillus niger* glucose oxidase (GOx) (A, pI 4.2) and the *Trichoderma reesei* proteins xylanase I (XYNI) (B), xylanase II (XYNII) (C) cellobiohydrolase I (CBHI) (D) and endoglucanase II (EGII) (E). The adsorption data on glucose oxidase binding to HFBI wild type layers was originally published by (Wang et al. 2010).

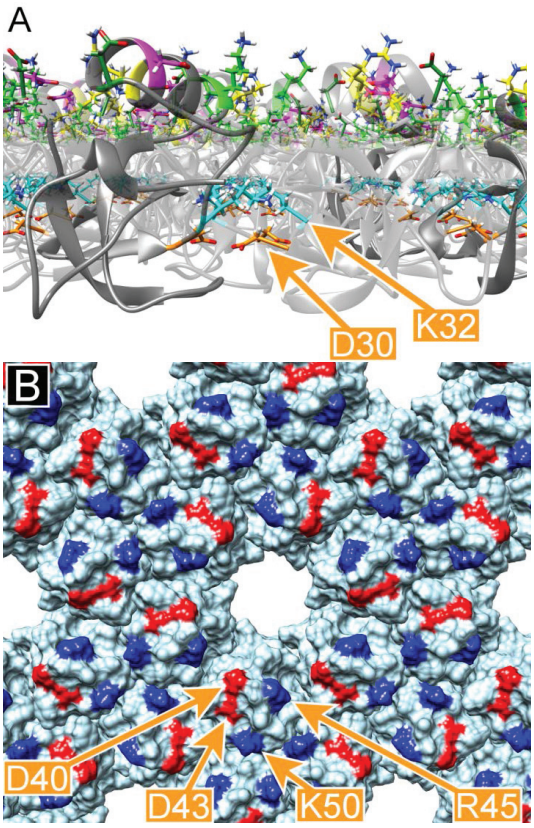

Figure 11. (A) side-view of a computational model of membrane formed by HFBI (Magarkar et al. 2014). Residues D30 and K32 are located within the membrane and are positioned so that they can form ionic bonds between HFBI molecules. (B) HFBI membrane viewed from its hydrophilic face. Residues D40, D43, R45 and K50 are exposed at the surface.

3.2.4 Formation of films at air-water interface

The behaviour of HFBI variants at the air-water interface displayed interesting properties. Firstly, the formation of a flattened plateau on top of a hydrophobin solution droplet was examined (II). The formation of plateau is a characteristic property of HFBI and is likely due to a formation of a hydrophobin monolayer at the air-water interface (Szilvay, Paananen, et al. 2007). All variants produced the same plateau forming effect, but at a varying time scale. For the wild type, the time formation was 19 ± 3.5 min, and for the variants the time was 30 – 70 % longer (Table 4).

Secondly, surface tension reduction upon HFBI layer formation on the air-water interface was measured using a Langmuir through in order to assess the protein concentration in the layers (II). In these measurements, there was little difference between the wild type (35.5 ± 1.6 mN) and the variants (Table 4).

The structure of hydrophobin films at the air-water interface has previously been examined by AFM (Szilvay, Paananen, et al. 2007). The authors showed that the film formed at the air-water interface by HFBI had a well ordered hexagonal structure and was represented by oligomer-like assemblies. The au-

thors further suggested that the hydrophobic patch would be faced towards the air-water interface and the hydrophilic side towards the aqueous environment. In this work, AFM measurements on HFBI variants was carried out similarly by transferring LB films of HFBI onto mica and following AFM measurements (II). All HFBI variants showed ordered structures (Figure 12) comparable to structures of wild-type HFBI (Szilvay, Paananen, et al. 2007). The raft-like structures seen in Figure 12 are likely artefacts of film transfer from larger crystalline domains formed in the air-water interface onto mica.

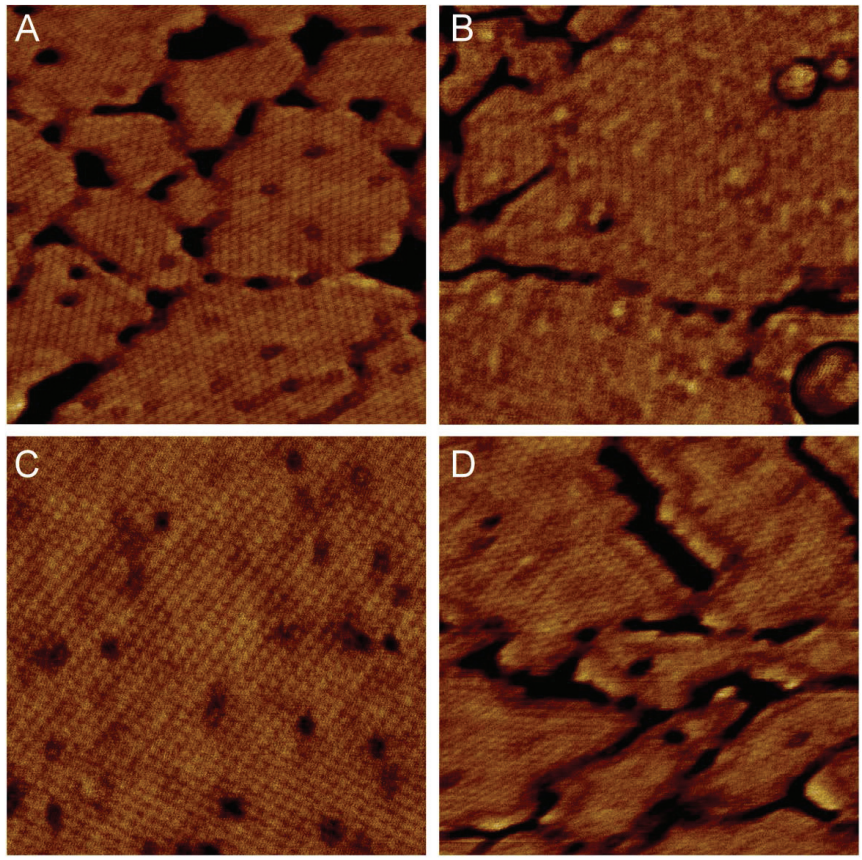

Figure 12. AFM images of LB-films of HFBI that were assembled at the air–water interface and have been transferred to a flat mica substrate, dried and imaged in air using tapping mode. Displayed are typical 200 nm phase images of the HFBI variants D30N/K32Q, D40Q/D43N, R45Q/K50Q and D40Q/D43N/R45Q/K50Q (A–D, respectively).

The clearest differences of hydrophobin films at the air-water interface comparing wild type HFBI and variants were seen examining interfacial rheology properties. The storage modulus (elastic, G′) and loss modulus (viscous, G″) of the hydrophobin layers were determined by interfacial shear rheology measurements (Figure 13). At equilibrium, G′ for the wild-type was 1.04 ± 0.01 N/m, the equilibrium values for variants D30N/K32Q, D40Q/D43N, R45Q/K50Q and D40Q/D43N/R45Q/K50Q were 0.85 ±0.10, 0.62 ±0.01, 1.44 ± 0.03 and 1.09 ± 0.01 N/m respectively (Figure 13A).

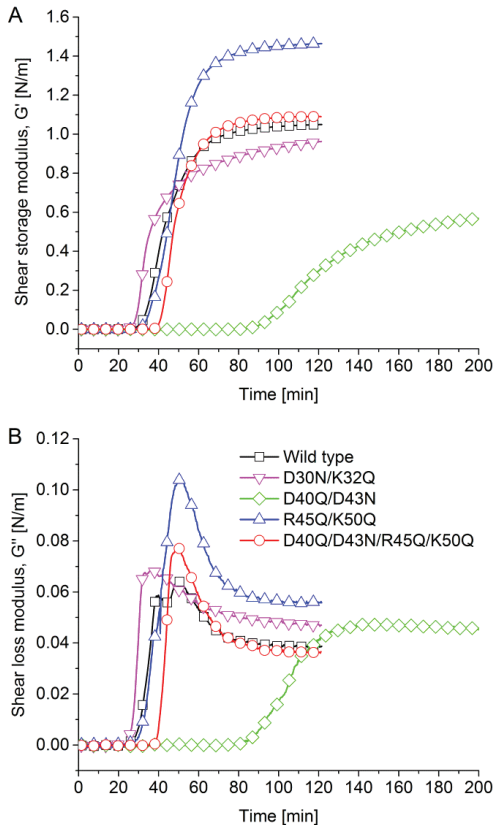

Figure 13. Interfacial rheology data (storage modulus, G' = A; loss modulus, G'' = B) of HFBI wild-type and HFBI variants D30N/K32Q, D40Q/D43N, R45Q/K50Q and D40Q/D43N/R45Q/K50Q at the air-water interface as a function of adsorption time. The interfacial layers are adsorbed from 0.3 μM protein solutions.

The equilibrium shear loss modulus values G″, were less than 0.06 N/m for all hydrophobins, at all cases lower than the G′ values, making them elastic in nature (Figure 13B). Variant R45Q/K50Q showed a ~40 % increase in G′ compared to wild-type. This value is as far as we understand the highest value of storage modulus for a protein film reported compared to literature (Cox et al. 2007). The overall high values of G′ for all variants and wild-type makes the protein films highly elastic. In all cases a remarkably long film formation lag time was detected before onset of significant increase of both G′ and G″. D30N/K32Q displayed the shortest lag time and D40Q/D43N displayed the longest. The overall rate of change was the slowest for D30N/K32Q. The loss modulus also increased the fastest for D30N/K32Q. D30 and K32, neutralized in the D30N/K32Q variant, are located near the hydrophobic patch, on the lateral side of the protein (Figure 8) and could participate in the formation of ionic bonds between molecules (II) . Following this, it is suggested that the residues D30N/K32Q have a role in the mechanism of initial docking in layer formation. Variant D40Q/D43N was showing the longest assembly times and lowest values of G′. Comparing this to the remarkably high G′ value of

R45Q/K50Q, it is interesting to note that the combination of these, where all charged residues have been neutralized, D40Q/D43N/R45Q/K50Q, led to a behaviour in terms of G′ that was close to the wild type and overall behaviour approximately as an average of D40Q/D43N and R45Q/K50Q.

In computational modelling of a membrane (Figure 11) these resiudes are all located on the hydrophilic part of the formed layer and thus not expected to be involved in direct molecular interactions as was suggested for D30N/K32Q. A reason for this could be that the hydrophilic face of the film interacts with other components on the water face. This could possibly be other hydrophobins, further supported by literature where a continuous dynamic state between interface assembled hydrophobin and hydrophobin in solution is presented (Krivosheeva et al. 2013). Furthermore, in publication III is was observed that about 10 % of a self-assembled layer of hydrophobin formed on HEX TMA was removed during washing, which could be composed of hydrophobins in dynamic exchange with the bound layer. As discussed earlier, structure and charge of the hydrophilic face of the hydrophobin layer is having an important role in recruiting a secondary layer of protein when adsorbed on a surface and it is possible that the same face could be interacting with other hydrophobins in solution when forming a layer in the air-water interface.

3.3 Hydrophobin Interactions with polar Surfaces (III)

In publication II it was shown that films formed by hydrophobins selectively bind to proteins and molecules via the hydrophilic side of the film. Furthermore, it has been shown that hydrophobins are involved in making spores and other fungal structures hydrophobic (Nakari-Setälä et al. 1997; Bell-Pedersen et al. 1992). In publication I at was also suggested that hydrophobins bind differently in terms of orientation on spherical surfaces with varying polarity. Following this, it his highly interesting to examine the role of the hydrophilic side of hydrophobins in mediating anchoring of the proteins on spores and cell walls and thereby rendering them hydrophobic, and to further examine the roles of charged residues on the hydrophilic side of the proteins in terms of interactions with polar surfaces. In order to examine these interesting properties, the abilities of hydrophobins to assemble onto solid polar hydrophilic surfaces in solution so that the hydrophobic side of the formed film would face outward towards solution were studied (III).

3.3.1 Interfacial assembly on polar surfaces

Hydrophobin adsorption to both cationic (TMA, PEI) and anionic (MUA) polar hydrophilic surfaces were examined using QCM-D. As a measure of hydrophobicity, the water contact angle (WCA) was measured on all surfaces before and after protein adsorption. The adsorption onto hydrophobic HEX surfaces was also measured. Representative QCM-D adsorption curves are shown in Figure 14.

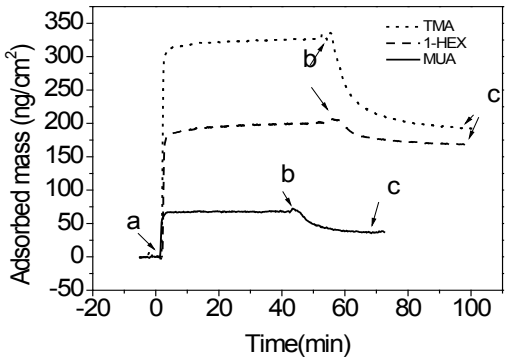

Figure 14. QCM-D sensogram graph showing representative curves of HFBI binding to different self-assembled monolayer (SAM) surfaces. The surfaces used were hydrophobic HEX (at pH 9.5), anionic MUA (at pH 9.0), and cationic TMA (at pH 9.0). Part a corresponds to hydrophobin injection, part b to buffer wash, and part c to end of buffer wash where adsorbed mass and WCA was measured. The adsorbed mass was calculated from resonance frequency change between the initial point (a) and the final point (c).

On cationic TMA surfaces, the protein adsorption of HFBI, HFBII and HFBII was measured by QCM-D over a pH range between 4.0 and 10.5 (Figure 15A). A negative control TMA surface was treated similarly, but without addition of protein. About half of the initially bound mass was typically removed from the surface during washing (Figure 14). The maximum adsorbed mass of HFBI (215 ng/cm^2) was obtained at pH 9.0, a value close to what is expected for a monolayer which has been approximated as 250 ng/cm^2 (Hakanpää 2006). HFBII and HFBII bound to the TMA layer, but at lower levels. The corresponding WCAs before and after hydrophobin coating are seen in Figure 15B. Water drop profiles corresponding to pHs with highest WCAs for each protein are presented in Figure 15D. The TMA surface had a WCA of about 22.3° ±5.7° before coating. All three proteins show a similar pH dependency on WCA, with a maximum peak at pH 8.0 -9.0 with WCAs clearly higher (60- 70°) that the buffer only sample (28 – 30°). Effect of type of buffer used WCA values was examined by measuring WCA on a narrow pH range with different buffers (Figure 15C). A minor buffer related effect was detected, (roughly 5°). The strong pH dependency indicates that electrostatic interactions are important for the interaction between hydrophobin layer and the polar, cationic surface.

Further examining the pH dependency of adsorption, HFBI and HFBII was also allowed to adsorb on hydrophobic HEX SAMs in the same PH range (Figure 16). Here it was expected that the hydrophobins interact with the surface via their hydrophobic patch (Wang et al. 2010) and as result the binding should show low pH dependency. It was observed that hydrophobin adsorbed between 170 and 282 ng/cm in the surface after about 10 % of binding was lost during the washing step. WCAs were measured as 39° and 56° and between38° and 50° for HFBI and HFBII respectively. Comparing these values to an uncoated reference HEX surface under the same condition, the hydrophobin adsorption made the surfaces clearly more hydrophilic indicating binding via the hydrophobic patch. The adsorption was non pH dependant as expected.

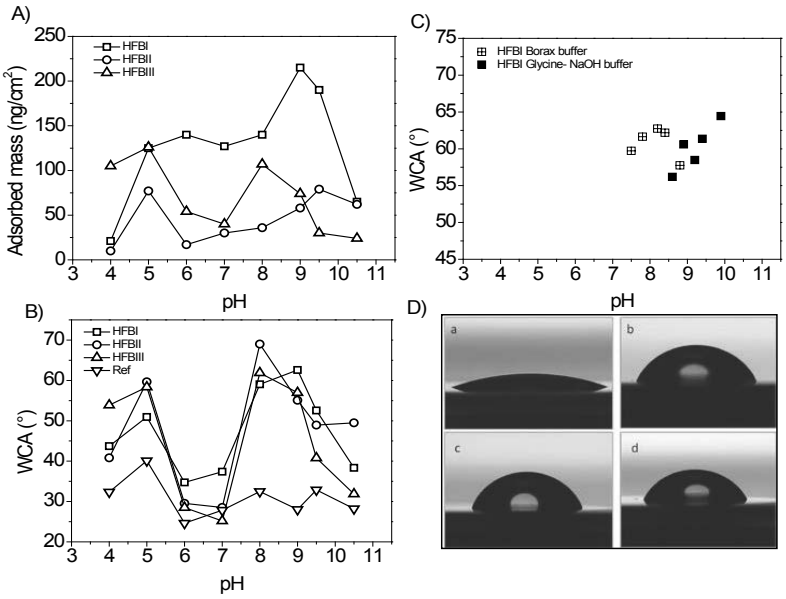

Figure 15. Adsorption of hydrophobins on cationic SAM surfaces. (A) QCM-D derived adsorbed mass of HFBI, HFBII, and HFBIII on TMA SAM surface as a function of pH. (B) WCAs of the same surfaces after hydrophobin adsorption in QCM-D runs as a function of pH. WCAs after HFBI, HFBII, or HFBIII adsorption are shown, as well as a negative control surface (labeled ref) that was treated similarly but without addition of protein. (C) WCA of HFBI on a TMA SAM surface at a narrow pH range. (D) Water drop profile shapes from WCA measurements on TMA SAM surfaces before protein coating (a), after HFBI (at pH 9.0) (b), HFBII (at pH 8.0) (c), and HFBIII (at pH 8.0) (d) coating. The obtained WCAs were 22.3° before deposition, and 62.6°, 69.0°, and 61.9°, after HFBI, HFBII, and HFBIII adsorption, respectively

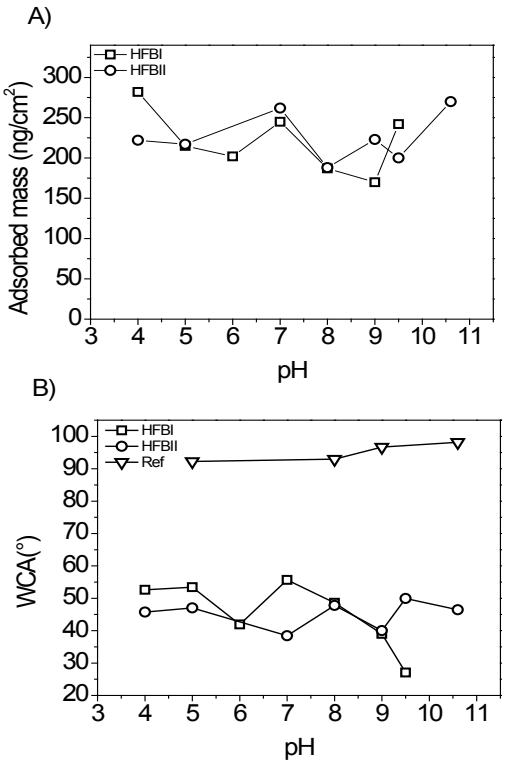

Figure 16. Adsorption of hydrophobins on hydrophobic surfaces. (A) Graph of adsorbed mass of HFBI and HFBII on hydrophobic HEX SAM as a function of pH as observed by QCM-D. (B) WCAs as a function of pH of the HEX SAM coated QCM-D sensors after HFBI or HFBII adsorption. A negative control surface (labeled ref) was treated similarly but without addition of protein. The standard deviation for HFBI on HEX SAM was ±6.7° (N =3) at pH 9.

In order to study the effect of the type of cationic surface, QCM-D and WCA experiments were repeated using HFBI on a structurally different surface, spin-coated cationic polymer PEI (Figure 17). The amount of HFBI adsorbed on the PEI surface (WCA 10° before deposition) as a function of pH shows a peak at pH 5.0 and a maximum binding at pH 10.0 where 260 ng/cm² was adsorbed. Also WCA values show two peaks, a smaller peak at pH 5.0 and a maximum peak at pH 8.0 (50.3°). Hydrophobin adsorption on PEI thus show binding and WCA similar to assembly on TMA as well as a similar pH dependency.

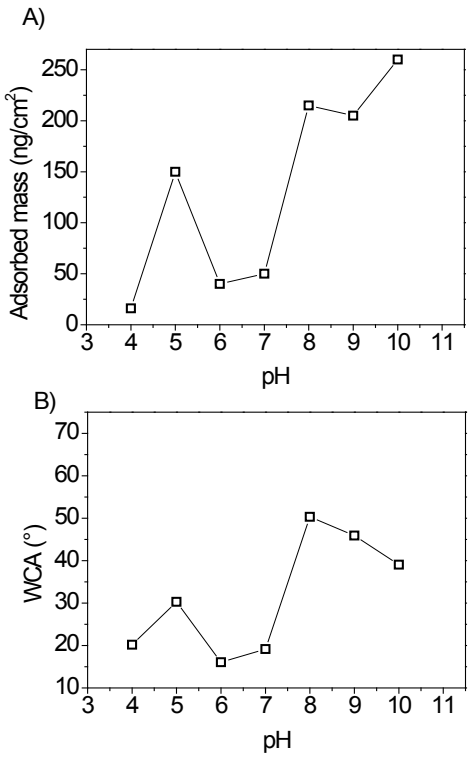

Figure 17. Adsorption of HFBI on cationic PEI surfaces. (A) Mass of adsorbed HFBI on cationic PEI surface as observed by QCM-D at various pHs. (B) WCAs of HFBI coatings on PEI after QCM-D measurements as a function of pH. The WCA of PEI surface before deposition was <10°.

Negatively charged SAM surfaces formed by 1-mercaptounedacanoic acid (MUA) was in a following step studied with QCM-D and WCA measurements to further examine the effect of charge on hydrophobin adsorption (Figure 18). At low pH, there was a significant protein binding with amounts close to a theoretical monolayer, but the binding rapidly decreased with increasing pH. The WCAs were however lower after HFBI adsorption compared to uncoated MUA SAM (31.5° ±3.3°) in the whole pH range. HFBI was thus showed to be inefficient to adsorb in anionic surfaces in order to change their polarity.

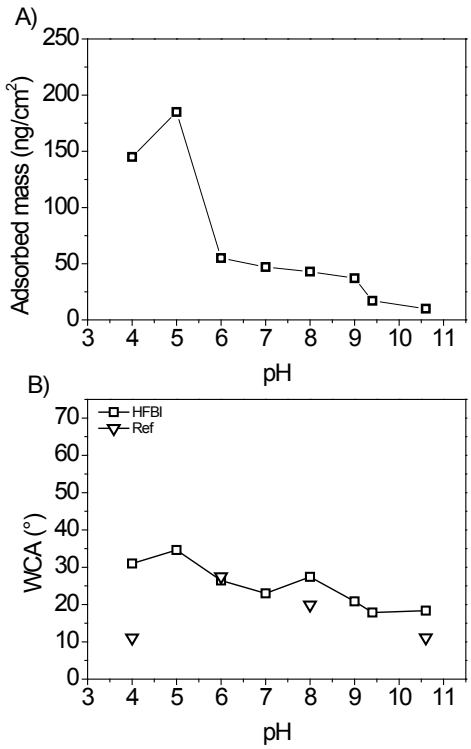

Figure 18. Adsorption of HFBI on anionic MUA SAM. (A) QCM-D derived mass of adsorbed HFBI on MUA as a function of pH. (B) WCAs of the same surface after HFBI adsorption as well as a negative control surface (labelled ref) that was treated similarly but without addition of protein are shown.

In order to further study the nature of interaction of HFBI on polar surfaces and the possible role of electrostatic interactions, HFBI was allowed to adsorb on TMA SAMs at increasing ionic strength using NaCl at different concentrations (0, 10, 25, 50, 75, 100, 500 mM) at pH 9.0 (Figure 19). Both bound mass and WCA was shown to rapidly decrease with increasing ionic strength, further indicating that electrostatic interactions are important for the interaction between hydrophobin layer and polar, cationic surface.

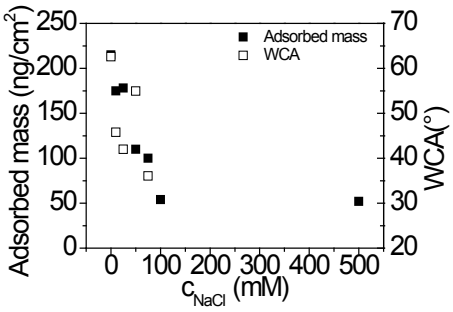

Figure 19. HFBI adsorption to cationic TMA SAMs as a function of NaCl concentration. QCM-D derived adsorbed mass and WCA are shown. The protein adsorption was done at pH 9.0

Hydrophobin was here observed to effectively change the polarity of both hydrophilic and hydrophobic surfaces through self-assembly in solution. Dependency on pH and ionic strength observed when adsorbing hydrophobins on polar cationic surfaces indicates that electrostatic interactions are important for the interaction between a hydrophobin layer and surfaces, especially as a similar pH dependency was not observed when adsorbing hydrophobin on a hydrophobic reference surface. Experiments in two structurally different anionic surfaces (TMA and PEI) generated very similar results and compared to very low binding on anionic surfaces, indicating that in this case, specific charge was very important. Interestingly, in publication II it was suggested that structure is important on recruiting proteins to the hydrophilic side of the film, and holes in the film has been suggested in modelling (II, Figure 11). AFM imaging on films formed on TMA SAM were made but specific features could not be seen other than the formation of a uniform layer (III).

The results shown here indicate that the layers formed by hydrophobins on surfaces with varying polarity are amphiphilic with one side giving a low contact angle and the other a high contact angle. When adsorbing on a hydrophobic surface, the hydrophilic side of the layer is turned towards the solution as has also been suggested previously for layers formed at the air-water interface (Szilvay, Paananen, et al. 2007). The presence of hydrophobin resulted in an increase of WCA of almost 40° after adsorption on a cationic surface suggesting that the hydrophobic patch, and the hydrophobic part of the adsorbed film, would be turned towards solution. Ionisable side chains are present on the hydrophilic part of HFBI, HFBII and HFBII surfaces (III), and the importance of pH and ionic strength seen here is likely a result of how these charged residues interact with the surface through electrostatic interactions. The charged residues of HFBI were shown to selectively bind to proteins and molecules via the hydrophilic side of the film in publication II. The results shown here further indicate that the charged residues are important for how the hydrophobins interact with their environment. Hydrophobins have been shown to be involved in making spores and other fungal structures hydrophobic (Nakari-Setälä et al. 1997; Bell-Pedersen et al. 1992) and the self-assembly in

solution described here is a possible mechanism on how hydrophobins assemble in fungal structures resulting in hydrophobic coatings. In publication I it was also suggested that hydrophobins bind differently in terms of orientation on spherical surfaces with varying polarity. Surface curvature and interactions with other proteins and molecules are likely also important in forming the highly hydrophobic fungal structures observed (Approximately 140°, Figure 1). The effect of poly- and monosaccharides on hydrophobin assembly have been observed (Armenante et al. 2010; Scholtmeijer et al. 2009) and hydrophobins can possibly interact with these to form hydrophobic coatings on fungal structures. Nonetheless it is shown that polar surfaces can act as support for amphiphilic hydrophobin membranes and thereby changing the polarity significantly.

3.4 Dynamics and interactions of hydrophobin assembly in solution (IV)

Little is known on the kinetics and thermodynamics of the self-association of hydrophobins in solution. In this work we examine these properties by stopped-flow fluorescence measurements (SF) and Förster Resonance Energy Transfer (FRET) giving an understanding in the process of hydrophobin solution multimer exchange and how the exchange is affected by environment on terms of other hydrophobins, proteins and surfactants (IV). The different types of multimers formed by class II hydrophobins in solution have been described previously. HFBI and HFBII have been shown to form dimers and tetramers (Torkkeli et al. 2002; Kisko et al. 2008) clustered together through their hydrophobic patches (Hakanpää et al. 2004; Hakanpää 2006). Multimerization of HFBI has been shown to be dependent on hydrophobin concentration and HFBI multimers have been shown to continuously disassemble and reassemble in solution. Furthermore, a continuous dynamic state between interface assembled hydrophobin and hydrophobin in solution has been suggested by (Krivosheeva et al. 2013).

3.4.1 Dynamics of hydrophobin multimer exchange

The dynamics of HFBII multimer exchange in solution was examined by Stopped-Flow spectroscopy (IV). A FRET pair of cy3 and cy5 labelled HFBII-CysC, donor and acceptor was used. The samples were prepared with a 1:10 ratio of labelled HFBII-CysC to unlabelled HFBII where each syringe was loaded with 10 μg/ml labelled HFBII and 90 μg/ml wild-type HFBII, with the cy3 in syringe 1 and cy5 label in syringe 2 resulting in a total HFBII concentration in each syringe of 100 μg/ml. 100 μg/ml total HFBII was set as reference. The addition of wild-type mas made in order to reduce the very high fluorescence signal as performed before (Szilvay et al. 2006) and the concentration dependency of FRET signal was controlled in SEC measurements (IV). Liquid from both syringes were simultaneously injected into a small cuvette after which the flow was stopped and the resulting fluorescence was measured. The

formation of FRET signal followed a single exponential curve showing the time dependence of multimer exchange.

Kinetics of hydrophobin multimer exchange was described with exchange half-life, $t_{1/2}$, and was attained from the FRET signal curve (example in Figure 20) fitted as single exponential, giving a $t_{1/2}$ for the exchange of 0.88 sec at 22°C (Table 5).

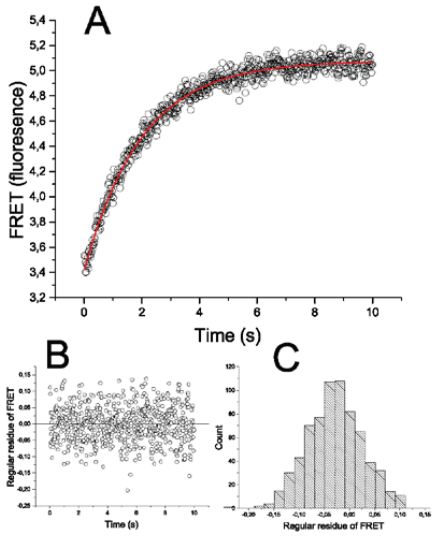

Figure 20. A) Fitting of a single exponential curve of the general form y = A*exp(-x/t1) + y0 to FRET data. B) Residuals show an even distribution throughout the time range of collecting data. C) Residuals have a normal distribution around the fitted curve.

The half-life of protein complexes have been studied previously (Table 5). These can be divided into two groups, a group with $t_{1/2}$ values of milliseconds and those with higher stability with corresponding $t_{1/2}$ values in minutes or hours, reflecting biological functionality. The disassociation of insulin dimers is several times faster, whereas an example of antibody self-association and DNA-binding protein disassociation are slower, with $t_{1/2}$ of about an hour and several minutes respectively. HFBII is placed between somewhere these groups, showing a much faster exchange rate than structural interactions, but still significantly slower than cases where exchange has a biological role. The relatively slow half-life of HFBII multimer exchange is suggested to reflect its biological function, where the multimer driving forces are strong and but still allow dynamic interactions in order to enable the multimer building blocks to take part in growth or surface interactions.

Table 5. Ea, $t_{1/2}$ diss for selected proteins including HFBII

Protein	Ea (kJ/mole)	$t_{1/2}$ diss.	Temp °C
HFBII multimer	92.51	0.88 sec	22
Insulin monomer-dimer (Koren & Hammes 1976)	10.5 ass. 30.9 diss.	6.08* 10^{-9} sec [a]	23
Phosphorylase b, two dimers to tetramer (Muñoz et al. 1983)	12.3 ass.[b] 32.3 diss.[b]	1.5 min [a]	25
Recombinant humanized antibody (rhuMAb) VEGF self-association (Moore et al. 1999)	45.2.	1 h [a]	30
Spectrin dimer – tetramer (Ungewickell & Gratzer 1978)	250.0 ass. 460.0 diss.	10 h [a]	29.5
Intermediate state of folding of Cytochrom C (Yeh et al. 1997)	50.0	0.04 sec [a]	20
Bence-Jones protein Au variable fragment dimerization (Maeda et al. 1978)	N/A	0.005 sec[a]	20
TATA binding protein (TBP) dimer dissacociate (Coleman & Pugh 1997)	N/A	7.4 min	25

Data has been converted to the appropriate units when necessary.[a] Calculated from $k_{diss.}$ assuming first order kinetics ($t_{1/2} = \ln(2)/k_{diss.}$) [b]Approximated using two-point Arrhenius.

Thermodynamics of the hydrophobin multimer exchange was measured by examining the temperature dependency of multimer exchange in SF at three temperatures, (21.5°, 17.5° and 12.5° C). The Arrhenius equation, k=Ae^(-Ea/RT) gives activation energy Ea and frequency factor A by plotting ln(k) vs. 1/T (K), where k is the reaction rate constant from fitting and T temperature (K), example in Figure 21. The activation energy of the HFBII multimer exchange was 92.5 kJ/mole which is in the lower range comparing to other protein complexes (Table 5), but multiple times larger than e.g. an antibody self-association process.

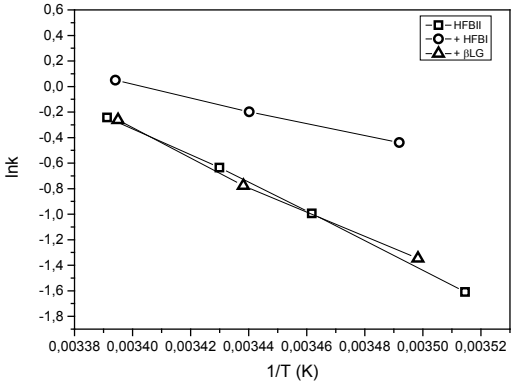

Figure 21. Example of plotting for Arrhenius calculation

3.4.2 Effect on hydrophobin multimer exchange by its surroundings

Addition of HFBI, milk proteins and surfactants was made in order to examine the role of the surroundings on HFBII multimer exchange. The effect on $t_{1/2}$ on

of the multimer exchange by these can be seen in Figure 22, and a comparison using extrapolated values at 20°C is seen in Table 6.

The small surfactant molecules Tween-20 (0.1 %) and Sodium dodecyl sulfate (SDS) (0.01 % in 1:20 labelled : non- labelled HFBII) as well as ethanol (5 %) affected the multimer exchange rate. Ethanol and Tween-20 considerably increased the rate of exchange as seen with lower $t_{1/2}$ values. Tween-20 is likely to interact with the hydrophobic patch of the proteins and ethanol has been shown to dissolve some of the aggregates formed by class II hydrophobins. It is suggested that these molecules are altering hydrophobic interactions in the multimers. The exchange is also shown to be affected by increased ionic strength (NaCl gradient 10, 50, 100 and 200 mM), with larger $t_{1/2}$ observed at higher concentration of NaCl, supporting this conclusion. Furthermore, if electrostatic interactions were involved in e.g. stabilising the complex, a destabilization of the complex and a lower $t_{1/2}$ as a result of salt increase is expected.

Addition of HFBI resulted in a significantly shorter $t_{1/2}$ for exchange in the whole temperature range while a corresponding addition of wild-type HFBII decreased the $t_{1/2}$ by much less, about 10 %. Activation energy also decreased considerably after addition of HFBI (Table 7). This suggests that an interaction between HFBI and HFBII is leading to a destabilization of the HFBII complex making the multimers reassemble at a faster rate. The biological significance of this interaction remains unclear but shows that hydrophobins interact with each other and clearly affect the behaviour of each other. The 10 % decrease in $t_{1/2}$, by doubling the concentration of HFBII indicates that a higher protein concentration to some extent affects how multimers are formed and disassembled, possible due to a shift of size distribution of multimers, e.g. from dimers to tetramers. These may have different rates of formation, but with the methods used here it was not possible to distinguish between these.

β-lactoglobulin and β-casein (1 mg/ml) did not affect the exchange showing that there is little or no interaction between these relative large molecules and the HFBII multimers.

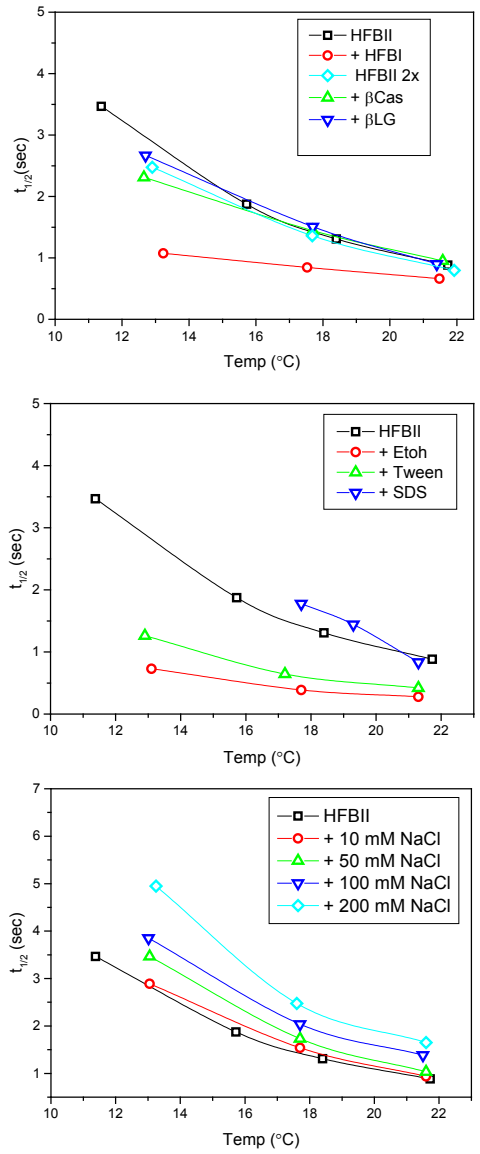

Figure 22. Top: Effect of HFBI,β-casein, β-lactoglobullin and HFBII 2x on t1/2 middle: effect of Tween (0.1 %), ethanol (5 %) and SDS (0.01 % in 1:20 labelled:unlabelled HFBII) on t1/2 bottom: Effect on t1/2 by increasing NaCl concentration.

Table 6. $t_{1/2}$ compared to HFBII reference case using extrapolated data at 20.0° C. Concentrations: Tween (0.1 %), ethanol (5 %) and SDS (0.01 % in 1:20 labelled:unlabelled HFBII) HFBII 100 µg/ml reference is also compared to HFBII 2x (200 µg/ml HFBII, 10 µg/ml labelled HFBII and 190 µg/ml wt HFBII)

	20,0°
HFBII	
+ HFBI	-32 %
HFBII 2x	-10 %
+ βCas	2 %
+ βLG	2 %
+ ethanol	-71 %
+ Tween-20	-55 %
+ SDS	5 %
+ Nacl (mM)	
10	5 %
50	16 %
100	49 %
200	78 %
Extrapolated values	

Table 7. Activation energies, frequency factors. Concentrations: Tween (0.1 %), and ethanol (5 %)

	Ea, kJ/mol	A (Freq. Factor), s^{-1}
HFBII	92.51	1.95E+16
+HFBI	41.38	2.26E+07
HFBII 2x	88.17	3.51E+15
+ βCAS	69.44	1.46E+12
+ βLG	86.83	1.88E+15
+ Etoh	83.38	1.60E+15
+ Tween-20	91.81	3.31E+16
+ Nacl (mM)		
10	92.42	1.77E+16
50	99.33	2.70E+17
100	84.88	5.72E+14
200	92.70	1.17E+16
Note: values for addition of SDS were not possible to obtain due to precipitation in the sample		

In summary the multimerization in solution of HFBII is shown to be a relatively slow exchange process between different multimers. An evident effect of the surroundings on multimer exchange and solution behaviour can be seen as small surfactant molecules as well as increased ionic strength is affecting the exchange rate showing that hydrophobic interactions are important in multimer formation. Commonly used milk proteins casein and β-lactoglobullin do not affect the rate of exchange. The interaction between HFBI and HFBII leads to a destabilization of the HFBII complex making the multimers reassemble at a faster rate, seen as a decrease in $t_{1/2}$, and show that the two hydrophobins interact and clearly affect the behaviour of each other.

4. Conclusions

The results presented here show that hydrophobins function by selectively interacting with their surroundings and that the surroundings in which the proteins exist also affects their function.

Hydrophobins strongly adhere to surfaces of varying polarity and structure by self-assembly, governed by their amphiphilic nature and adsorb with different orientation on hydrophilic and hydrophobic surfaces (I, III). The proteins selectively recruit other proteins and molecules to a self-assembled amphiphilic film of hydrophobin (I, II). Their structure and charged residues are shown to be responsible for these selective interactions. HFBI variants bound to a surface are shown to recruit *T. reesei* enzymes specifically depending on local protein surface charge on the hydrophilic part of the protein (II), and HFBII adsorbed on NPs was shown to adsorb layers of human plasma proteins in different manner when adsorbed on NPs of varying polarity (I). Surface films formed by hydrophobins are highly elastic, and charged residues on the side of the proteins have a role in stabilizing the protein films formed (III). Charged residues located on the hydrophilic part of the formed self-assembled film are suggested as being in a dynamic state with hydrophobins and other proteins and molecules in solution (II, III).

The surroundings in which the proteins exist affect their function. Surfaces of varying polarity in the protein surroundings affect how the proteins self-assemble (I, III). Hydrophobin multimer exchange in solution is shown to be governed by hydrophobic interactions and the multimer exchange behaviour is affected by other proteins and molecules, such as small surfactants and salt interacting with the hydrophobic patch of the proteins, and HFBII and HFBI are shown to interact in solution altering multimer kinetics and thermodynamics considerably (IV).

The specific recruiting and self-assembly behaviour of the proteins depending on polarity shown here gives excellent opportunities for hydrophobin use in specialised coatings on biocompatible implants, self-assembled and anchoring layers on biosensors, and e.g. nanoparticles for drug delivery coated with a hydrophobic coating specifically via secondary binding. Increased knowledge in what type of molecules affect the dynamics of hydrophobin multimer exchange can e.g. be used to make stabilized hydrophobic emulsions in food- and pharmaceutical industry with increased specificity.

The knowledge learned here regarding hydrophobins show that these proteins can be specialised to function as highly selective self-assembling building

blocks, and is enabling development of practical and specific implementations utilizing of a group of common proteins with extraordinary properties.

References

Aimanianda, V. et al., 2009. Surface hydrophobin prevents immune recognition of airborne fungal spores. *Nature*, 460(7259), pp.1117–21. Available at: http://dx.doi.org/10.1038/nature08264 [Accessed March 8, 2015].

Armenante, A. et al., 2010. The Pleurotus ostreatus hydrophobin Vmh2 and its interaction with glucans. *Glycobiology*, 20(5), pp.594–602. Available at: http://www.ncbi.nlm.nih.gov/pubmed/20100692 [Accessed June 1, 2015].

Askolin, S. et al., 2006. Interaction and comparison of a class I hydrophobin from Schizophyllum commune and class II hydrophobins from Trichoderma reesei. *Biomacromolecules*, 7(4), pp.1295–301. Available at: http://www.ncbi.nlm.nih.gov/pubmed/16602752 [Accessed May 31, 2015].

Askolin, S. et al., 2005. The Trichoderma reesei hydrophobin genes hfb1 and hfb2 have diverse functions in fungal development. *FEMS microbiology letters*, 253(2), pp.281–8. Available at: http://www.sciencedirect.com/science/article/pii/S037810970500683X [Accessed May 23, 2015].

Bailey, M.J. et al., 2002. Process technological effects of deletion and amplification of hydrophobins I and II in transformants of Trichoderma reesei. *Applied microbiology and biotechnology*, 58(6), pp.721–7. Available at: http://www.ncbi.nlm.nih.gov/pubmed/12021790 [Accessed May 30, 2015].

Bell-Pedersen, D., Dunlap, J.C. & Loros, J.J., 1992. The Neurospora circadian clock-controlled gene, ccg-2, is allelic to eas and encodes a fungal hydrophobin required for formation of the conidial rodlet layer. *Genes & development*, 6(12A), pp.2382–94. Available at: http://www.ncbi.nlm.nih.gov/pubmed/1459460 [Accessed May 23, 2015].

Bilewicz, R. et al., 2001. Modification of Electrodes with Self-Assembled Hydrophobin Layers. *The Journal of Physical Chemistry B*, 105(40), pp.9772–9777. Available at: http://dx.doi.org/10.1021/jp0113782 [Accessed May 28, 2015].

Bruns, S. et al., 2010. Production of extracellular traps against Aspergillus fumigatus in vitro and in infected lung tissue is dependent on invading neutrophils and influenced by hydrophobin RodA. *PLoS pathogens*, 6(4), p.e1000873. Available at: http://www.pubmedcentral.nih.gov/articlerender.fcgi?artid=2861696&tool=pmcentrez&rendertype=abstract [Accessed May 23, 2015].

Clegg, R.M., 1992. Fluorescence resonance energy transfer and nucleic acids. *Methods in enzymology*, 211, pp.353–88. Available at: http://www.ncbi.nlm.nih.gov/pubmed/1406315 [Accessed April 19, 2015].

Coleman, R.A. & Pugh, B.F., 1997. Slow dimer dissociation of the TATA binding protein dictates the kinetics of DNA binding. *Proceedings of the National Academy of Sciences of the United States of America*, 94(14), pp.7221–6. Available at: http://www.pubmedcentral.nih.gov/articlerender.fcgi?artid=23798&tool=pmcentrez&rendertype=abstract [Accessed June 1, 2015].

Corvis, Y. et al., 2006. Analytical investigation of the interactions between SC3 hydrophobin and lipid layers: elaborating of nanostructured matrixes for immobilizing redox systems. *Analytical chemistry*, 78(14), pp.4850–64. Available at: http://www.ncbi.nlm.nih.gov/pubmed/16841903 [Accessed May 28, 2015].

Corvis, Y. et al., 2005. Preparing catalytic surfaces for sensing applications by immobilizing enzymes via hydrophobin layers. *Analytical chemistry*, 77(6), pp.1622–30. Available at: http://www.ncbi.nlm.nih.gov/pubmed/15762565 [Accessed May 31, 2015].

Cox, A.R. et al., 2007. Surface properties of class II hydrophobins from Trichoderma reesei and influence on bubble stability. *Langmuir*, 23(15), pp.7995–8002.

Cox, A.R., Aldred, D.L. & Russell, A.B., 2009. Exceptional stability of food foams using class II hydrophobin HFBII. *Food Hydrocolloids*, 23(2), pp.366–376. Available at: http://www.researchgate.net/publication/223162311_Exceptional_stability_of_food_foams_using_class_II_hydrophobin_HFBII [Accessed April 7, 2015].

Fan, H. et al., 2006. Molecular dynamics simulations of the hydrophobin SC3 at a hydrophobic/hydrophilic interface. *Proteins*, 64(4), pp.863–73. Available at: http://www.ncbi.nlm.nih.gov/pubmed/16770796 [Accessed May 25, 2015].

Fang, G. et al., 2014. Novel hydrophobin-coated docetaxel nanoparticles for intravenous delivery: in vitro characteristics and in vivo performance. *European journal of pharmaceutical sciences : official journal of the European Federation for Pharmaceutical Sciences*, 60, pp.1–9. Available at: http://www.ncbi.nlm.nih.gov/pubmed/24815943 [Accessed May 31, 2015].

Geisse, N.A., 2009. AFM and combined optical techniques. *Materials Today*, 12(7-8), pp.40–45. Available at: http://www.sciencedirect.com/science/article/pii/S1369702109702019 [Accessed April 12, 2015].

De Groot, P.W. et al., 1997. Isolation of developmentally regulated genes from the edible mushroom Agaricus bisporus. *Microbiology (Reading, England)*, 143 (Pt 6, pp.1993–2001. Available at: http://www.ncbi.nlm.nih.gov/pubmed/9202475 [Accessed May 23, 2015].

Gruner, M.S. et al., 2012. Self-assembly of class II hydrophobins on polar surfaces. *Langmuir*, 28(9), pp.4293–4300. Available at: http://www.ncbi.nlm.nih.gov/pubmed/22315927.

Haas Jimoh Akanbi, M. et al., 2010. Use of hydrophobins in formulation of water insoluble drugs for oral administration. *Colloids and surfaces. B, Biointerfaces*, 75(2), pp.526–31. Available at: http://www.sciencedirect.com/science/article/pii/S0927776509004639 [Accessed May 27, 2015].

Hakanpää, J. et al., 2004. Atomic resolution structure of the HFBII hydrophobin, a self-assembling amphiphile. *The Journal of biological chemistry*, 279(1), pp.534–9. Available at: http://www.ncbi.nlm.nih.gov/pubmed/14555650 [Accessed May 3, 2015].

Hakanpää, J., 2006. Two crystal structures of Trichoderma reesei hydrophobin HFBI--The structure of a protein amphiphile with and without detergent interaction. *Protein Science*, 15(9), pp.2129–2140. Available at: http://www.pubmedcentral.nih.gov/articlerender.fcgi?artid=2242604&tool=pmcentrez&rendertype=abstract [Accessed April 19, 2015].

Hou, S. et al., 2008. Patterning of cells on functionalized poly(dimethylsiloxane) surface prepared by hydrophobin and collagen modification. *Biosensors & bioelectronics*, 24(4), pp.918–22. Available at: http://www.ncbi.nlm.nih.gov/pubmed/18782664 [Accessed May 31, 2015].

Hou, S. et al., 2009. Surface modification using a novel type I hydrophobin HGFI. *Analytical and bioanalytical chemistry*, 394(3), pp.783–9. Available at: http://www.ncbi.nlm.nih.gov/pubmed/19370343 [Accessed May 31, 2015].

Janssen, M.I. et al., 2002. Coating with genetic engineered hydrophobin promotes growth of fibroblasts on a hydrophobic solid. *Biomaterials*, 23(24), pp.4847–54. Available at: http://www.ncbi.nlm.nih.gov/pubmed/12361625 [Accessed May 31, 2015].

Kallio, J.M., Linder, M.B. & Rouvinen, J., 2007. Crystal structures of hydrophobin HFBII in the presence of detergent implicate the formation of fibrils and monolayer films. *The Journal of biological chemistry*, 282(39), pp.28733–9. Available at: http://www.ncbi.nlm.nih.gov/pubmed/17636262 [Accessed May 25, 2015].

Kazmierczak, P. et al., 2005. A Hydrophobin of the chestnut blight fungus, Cryphonectria parasitica, is required for stromal pustule eruption. *Eukaryotic cell*, 4(5), pp.931–6. Available at: http://www.pubmedcentral.nih.gov/articlerender.fcgi?artid=1140098&tool=pmcentrez&rendertype=abstract [Accessed May 23, 2015].

Kisko, K. et al., 2008. Interactions of hydrophobin proteins in solution studied by small-angle X-ray scattering. *Biophysical journal*, 94(1), pp.198–206. Available at: http://www.pubmedcentral.nih.gov/articlerender.fcgi?artid=2134873&tool=pmcentrez&rendertype=abstract [Accessed May 25, 2015].

Kisko, K. et al., 2005. Langmuir–Blodgett films of hydrophobins HFBI and HFBII. *Surface Science*, 584(1), pp.35–40. Available at: http://www.sciencedirect.com/science/article/pii/S0039602805003651 [Accessed May 25, 2015].

Kisko, K. et al., 2007. Self-assembled films of hydrophobin protein HFBIII from Trichoderma reesei. *Journal of Applied Crystallography*, 40(s1), pp.s355–s360. Available at: http://scripts.iucr.org/cgi-bin/paper?aj6012 [Accessed May 25, 2015].

Koren, R. & Hammes, G.G., 1976. A kinetic study of protein-protein interactions. *Biochemistry*, 15(5), pp.1165–1171. Available at: http://dx.doi.org/10.1021/bi00650a032 [Accessed May 2, 2015].

Kostiainen, M.A. et al., 2006. Multivalent dendrons for high-affinity adhesion of proteins to DNA. *Angewandte Chemie (International ed. in English)*, 45(21), pp.3538–42. Available at: http://www.ncbi.nlm.nih.gov/pubmed/16639766 [Accessed May 31, 2015].

Krivosheeva, O. et al., 2013. Kinetic and equilibrium aspects of adsorption and desorption of class II hydrophobins HFBI and HFBII at silicon oxynitride/water and air/water interfaces. *Langmuir : the ACS journal of surfaces and colloids*, 29(8), pp.2683–91. Available at: http://dx.doi.org/10.1021/la3048888 [Accessed May 29, 2015].

Kwan, A.H.Y. et al., 2006. Structural basis for rodlet assembly in fungal hydrophobins. *Proceedings of the National Academy of Sciences of the United States of America*, 103(10), pp.3621–6. Available at:

http://www.pubmedcentral.nih.gov/articlerender.fcgi?artid=1533775&tool=pmcentrez&rendertype=abstract [Accessed May 25, 2015].

Kyte, J. & Doolittle, R.F., 1982. A simple method for displaying the hydropathic character of a protein. *Journal of Molecular Biology*, 157(1), pp.105–132. Available at: http://www.sciencedirect.com/science/article/pii/0022283682905150 [Accessed November 10, 2014].

Laaksonen, P. et al., 2010. Interfacial engineering by proteins: exfoliation and functionalization of graphene by hydrophobins. *Angewandte Chemie (International ed. in English)*, 49(29), pp.4946–9. Available at: http://www.ncbi.nlm.nih.gov/pubmed/20533486 [Accessed May 31, 2015].

Laaksonen, P. et al., 2009. Selective nanopatterning using citrate-stabilized Au nanoparticles and cystein-modified amphiphilic protein. *Langmuir : the ACS journal of surfaces and colloids*, 25(9), pp.5185–92. Available at: http://www.ncbi.nlm.nih.gov/pubmed/19253945 [Accessed May 31, 2015].

Linder, M. et al., 2002. Surface adhesion of fusion proteins containing the hydrophobins HFBI and HFBII from Trichoderma reesei. *Protein Sci*, 11(9), pp.2257–2266. Available at: http://www.ncbi.nlm.nih.gov/pubmed/12192081.

Linder, M. et al., 2001. The hydrophobins HFBI and HFBII from Trichoderma reesei showing efficient interactions with nonionic surfactants in aqueous two-phase systems. *Biomacromolecules*, 2(2), pp.511–7. Available at: http://www.ncbi.nlm.nih.gov/pubmed/11749214 [Accessed April 19, 2015].

Linder, M.B., 2009. Hydrophobins: Proteins that self assemble at interfaces. *Current Opinion in Colloid & Interface Science*, 14(5), pp.356–363. Available at: http://www.sciencedirect.com/science/article/pii/S1359029409000296 [Accessed March 29, 2015].

Linder, M.B. et al., 2005. Hydrophobins: the protein-amphiphiles of filamentous fungi. *FEMS microbiology reviews*, 29(5), pp.877–96. Available at: http://www.sciencedirect.com/science/article/pii/S0168644505000100 [Accessed May 24, 2015].

Ling, X.Y., Reinhoudt, D.N. & Huskens, J., 2008. Reversible Attachment of Nanostructures at Molecular Printboards through Supramolecular Glue. *Chemistry of Materials*, 20(11), pp.3574–3578. Available at: http://dx.doi.org/10.1021/cm703597w [Accessed May 28, 2015].

Lugones, L.G. et al., 1996. An abundant hydrophobin (ABH1) forms hydrophobic rodlet layers in Agaricus bisporus fruiting bodies. *Microbiology (Reading, England)*, 142 (Pt 5, pp.1321–9. Available at: http://www.ncbi.nlm.nih.gov/pubmed/8704971 [Accessed May 23, 2015].

Lugones, L.G. et al., 1999. Hydrophobins line air channels in fruiting bodies of Schizophyllum commune and Agaricus bisporus. *Mycological Research*, 103(5), pp.635–640. Available at: http://www.sciencedirect.com/science/article/pii/S0953756208603172 [Accessed May 23, 2015].

Lugones, L.G. et al., 2004. The SC15 protein of Schizophyllum commune mediates formation of aerial hyphae and attachment in the absence of the SC3 hydrophobin. *Molecular microbiology*, 53(2), pp.707–16. Available at: http://www.ncbi.nlm.nih.gov/pubmed/15228546 [Accessed May 23, 2015].

Lumsdon, S.O., Green, J. & Stieglitz, B., 2005. Adsorption of hydrophobin proteins at hydrophobic and hydrophilic interfaces. *Colloids and surfaces. B, Biointerfaces*, 44(4), pp.172–8. Available at: http://www.ncbi.nlm.nih.gov/pubmed/16085399 [Accessed March 29, 2015].

Mackay, J.P. et al., 2001. The Hydrophobin EAS Is Largely Unstructured in Solution and Functions by Forming Amyloid-Like Structures. *Structure*, 9(2), pp.83–91. Available at: http://www.sciencedirect.com/science/article/pii/S0969212600005591 [Accessed May 31, 2015].

Maeda, H., Steffen, E. & Engel, J., 1978. Kinetics of dimerization of the Bence-Jones protein Au. *Biophysical chemistry*, 9(1), pp.57–64. Available at: http://www.ncbi.nlm.nih.gov/pubmed/753404 [Accessed June 1, 2015].

Magarkar, A. et al., 2014. Hydrophobin film structure for HFBI and HFBII and mechanism for accelerated film formation. *PLoS computational biology*, 10(7), p.e1003745. Available at: http://journals.plos.org/ploscompbiol/article?id=10.1371/journal.pcbi.1003745 [Accessed May 27, 2015].

Mankel, A., Krause, K. & Kothe, E., 2002. Identification of a hydrophobin gene that is developmentally regulated in the ectomycorrhizal fungus Tricholoma terreum. *Applied and environmental microbiology*, 68(3), pp.1408–13. Available at: http://www.pubmedcentral.nih.gov/articlerender.fcgi?artid=123729&tool=pmcentrez&rendertype=abstract [Accessed May 23, 2015].

Misra, R. et al., 2006. Nanoscale reduction in surface friction of polymer surfaces modified with Sc3 hydrophobin from Schizophyllum commune. *Biomacromolecules*, 7(5), pp.1463–70. Available at: http://www.ncbi.nlm.nih.gov/pubmed/16677027 [Accessed May 31, 2015].

Monopoli, M.P. et al., 2011. Physical-chemical aspects of protein corona: relevance to in vitro and in vivo biological impacts of nanoparticles. *Journal of the American Chemical Society*, 133(8), pp.2525–34. Available at: http://dx.doi.org/10.1021/ja107583h [Accessed August 10, 2015].

Moore, J.M., Patapoff, T.W. & Cromwell, M.E., 1999. Kinetics and thermodynamics of dimer formation and dissociation for a recombinant humanized monoclonal antibody to vascular endothelial growth factor. *Biochemistry*, 38(42), pp.13960–13967.

Muñoz, F. et al., 1983. Kinetic and thermodynamic study of the tetramerization equilibrium of phosphorylase b. *Journal of biochemistry*, 94(5), pp.1649–59. Available at: http://www.ncbi.nlm.nih.gov/pubmed/6418736 [Accessed May 30, 2015].

Nakari-Setälä, T. et al., 1997. Differential expression of the vegetative and spore-bound hydrophobins of Trichoderma reesei--cloning and characterization of the hfb2 gene. *European journal of biochemistry / FEBS*, 248(2), pp.415–23. Available at: http://www.ncbi.nlm.nih.gov/pubmed/9346297 [Accessed May 29, 2015].

Paananen, A. et al., 2003. Structural hierarchy in molecular films of two class II hydrophobins. *Biochemistry*, 42(18), pp.5253–8. Available at: http://www.ncbi.nlm.nih.gov/pubmed/12731866 [Accessed May 25, 2015].

Palomo, J.M. et al., 2003. Solid-phase handling of hydrophobins: immobilized hydrophobins as a new tool to study lipases. *Biomacromolecules*, 4(2), pp.204–10. Available at: http://dx.doi.org/10.1021/bm020071l [Accessed May 28, 2015].

Paris, S. et al., 2003. Conidial Hydrophobins of Aspergillus fumigatus. *Applied and Environmental Microbiology*, 69(3), pp.1581–1588. Available at: http://aem.asm.org/content/69/3/1581.abstract [Accessed April 5, 2015].

Qin, M. et al., 2007. Bioactive surface modification of mica and poly(dimethylsiloxane) with hydrophobins for protein immobilization. *Langmuir : the ACS journal of surfaces and colloids*, 23(8), pp.4465–71. Available at: http://www.ncbi.nlm.nih.gov/pubmed/17341100 [Accessed May 28, 2015].

Rillig, M.C., 2005. A connection between fungal hydrophobins and soil water repellency? *Pedobiologia*, 49(5), pp.395–399. Available at: http://www.sciencedirect.com/science/article/pii/S0031405605000351 [Accessed May 23, 2015].

Rillig, M.C. et al., 2007. Role of proteins in soil carbon and nitrogen storage: controls on persistence. *Biogeochemistry*, 85(1), pp.25–44. Available at: http://link.springer.com/10.1007/s10533-007-9102-6 [Accessed May 23, 2015].

Sarlin, T. et al., 2005. Fungal Hydrophobins as Predictors of the Gushing Activity of Malt. *Journal of the Institute of Brewing*, 111(2), pp.105–111. Available at: http://doi.wiley.com/10.1002/j.2050-0416.2005.tb00655.x [Accessed May 31, 2015].

Sarparanta, M. et al., 2012. Intravenous delivery of hydrophobin-functionalized porous silicon nanoparticles: stability, plasma protein adsorption and biodistribution. *Molecular pharmaceutics*, 9(3), pp.654–63. Available at: http://www.ncbi.nlm.nih.gov/pubmed/22277076 [Accessed May 31, 2015].

Scherrer, S. et al., 2000. Interfacial self-assembly of fungal hydrophobins of the lichen-forming ascomycetes Xanthoria parietina and X. ectaneoides. *Fungal genetics and biology : FG & B*, 30(1), pp.81–93. Available at: http://www.ncbi.nlm.nih.gov/pubmed/10955910 [Accessed May 23, 2015].

Scholtmeijer, K. et al., 2009. Assembly of the fungal SC3 hydrophobin into functional amyloid fibrils depends on its concentration and is promoted by cell wall polysaccharides. *The Journal of biological chemistry*, 284(39), pp.26309–14. Available at: http://www.pubmedcentral.nih.gov/articlerender.fcgi?artid=2785318&tool=pmcentrez&rendertype=abstract [Accessed June 1, 2015].

Scholtmeijer, K. et al., 2002. Surface modifications created by using engineered hydrophobins. *Applied and environmental microbiology*, 68(3), pp.1367–73. Available at: http://www.pubmedcentral.nih.gov/articlerender.fcgi?artid=123772&tool=pmcentrez&rendertype=abstract [Accessed May 28, 2015].

Shapiro, A.L., Viñuela, E. & V. Maizel, J., 1967. Molecular weight estimation of polypeptide chains by electrophoresis in SDS-polyacrylamide gels. *Biochemical and Biophysical Research Communications*, 28(5), pp.815–820. Available at: http://www.sciencedirect.com/science/article/pii/0006291X67903919 [Accessed January 10, 2015].

Shibuya, K. et al., 1999. Histopathology of experimental invasive pulmonary aspergillosis in rats: pathological comparison of pulmonary lesions induced by specific virulent factor deficient mutants. *Microbial pathogenesis*, 27(3), pp.123–31. Available at: http://www.ncbi.nlm.nih.gov/pubmed/10455003 [Accessed May 23, 2015].

Spanu, P., 1997. HCF-1, a hydrophobin from the tomato pathogen Cladosporium fulvum. *Gene*, 193(1), pp.89–96. Available at: http://www.ncbi.nlm.nih.gov/pubmed/9249071 [Accessed May 23, 2015].

St Leger, R.J., Staples, R.C. & Roberts, D.W., 1992. Cloning and regulatory analysis of starvation-stress gene, ssgA, encoding a hydrophobin-like protein from the entomopathogenic fungus, Metarhizium anisopliae. *Gene*, 120(1), pp.119–24. Available at: http://www.ncbi.nlm.nih.gov/pubmed/1398117 [Accessed May 23, 2015].

De Stefano, L. et al., 2008. Protein-Modified Porous Silicon Nanostructures. *Advanced Materials*, 20(8), pp.1529–1533. Available at: http://doi.wiley.com/10.1002/adma.200702454 [Accessed May 31, 2015].

De Stefano, L. et al., 2007. Self-assembled biofilm of hydrophobins protects the silicon surface in the KOH wet etch process. *Langmuir : the ACS journal of surfaces and colloids*, 23(15), pp.7920–2. Available at: http://www.ncbi.nlm.nih.gov/pubmed/17580922 [Accessed June 5, 2015].

Stringer, M.A. et al., 1991. Rodletless, a new Aspergillus developmental mutant induced by directed gene inactivation. *Genes & development*, 5(7), pp.1161–71. Available at: http://www.ncbi.nlm.nih.gov/pubmed/2065971 [Accessed May 23, 2015].

Szilvay, G.R., Paananen, A., et al., 2007. Self-assembled hydrophobin protein films at the air-water interface: structural analysis and molecular engineering. *Biochemistry*, 46(9), pp.2345–54. Available at: http://dx.doi.org/10.1021/bi602358h [Accessed May 25, 2015].

Szilvay, G.R., Kisko, K., et al., 2007. The relation between solution association and surface activity of the hydrophobin HFBI from Trichoderma reesei. *FEBS letters*, 581(14), pp.2721–6. Available at: http://www.ncbi.nlm.nih.gov/pubmed/17531982 [Accessed May 31, 2015].

Szilvay, G.R., Nakari-Setälä, T. & Linder, M.B., 2006. Behavior of Trichoderma reesei hydrophobins in solution: Interactions, dynamics, and multimer formation. *Biochemistry*, 45(28), pp.8590–8598.

Tagu, D. et al., 2001. Immunolocalization of hydrophobin HYDPt-1 from the ectomycorrhizal basidiomycete Pisolithus tinctorius during colonization of Eucalyptus globulus roots. *New Phytologist*, 149(1), pp.127–135. Available at: http://doi.wiley.com/10.1046/j.1469-8137.2001.00009.x [Accessed May 23, 2015].

Tagu, D., Nasse, B. & Martin, F., 1996. Cloning and characterization of hydrophobins-encoding cDNAs from the ectomycorrhizal Basidiomycete Pisolithus tinctorius. *Gene*, 168(1), pp.93–97. Available at: http://www.sciencedirect.com/science/article/pii/0378111995007253 [Accessed May 23, 2015].

Takahashi, T. et al., 2005. The fungal hydrophobin RolA recruits polyesterase and laterally moves on hydrophobic surfaces. *Molecular microbiology*, 57(6), pp.1780–96. Available at: http://www.ncbi.nlm.nih.gov/pubmed/16135240 [Accessed May 28, 2015].

Talbot, N.J. et al., 1996. MPG1 Encodes a Fungal Hydrophobin Involved in Surface Interactions during Infection-Related Development of Magnaporthe grisea. *The Plant cell*, 8(6), pp.985–999. Available at: http://www.pubmedcentral.nih.gov/articlerender.fcgi?artid=161153&tool=pmcentrez&rendertype=abstract [Accessed May 23, 2015].

Talbot, N.J., Ebbole, D.J. & Hamer, J.E., 1993. Identification and characterization of MPG1, a gene involved in pathogenicity from the rice blast fungus Magnaporthe grisea. *The Plant cell*, 5(11), pp.1575–90. Available at: http://www.plantcell.org/content/5/11/1575.abstract [Accessed May 23, 2015].

Temple, B. et al., 1997. Cerato-ulmin, a hydrophobin secreted by the causal agents of Dutch elm disease, is a parasitic fitness factor. *Fungal genetics and biology : FG & B*, 22(1), pp.39–53. Available at: http://www.ncbi.nlm.nih.gov/pubmed/9344630 [Accessed May 23, 2015].

Torkkeli, M. et al., 2002. Aggregation and self-assembly of hydrophobins from Trichoderma reesei: low-resolution structural models. *Biophysical journal*, 83(4), pp.2240–7. Available at: http://www.pubmedcentral.nih.gov/articlerender.fcgi?artid=1302312&tool=pmcentrez&rendertype=abstract [Accessed May 25, 2015].

Ulman, A., 1996. Formation and Structure of Self-Assembled Monolayers. *Chemical reviews*, 96(4), pp.1533–1554. Available at: http://www.ncbi.nlm.nih.gov/pubmed/11848802 [Accessed June 2, 2015].

Ungewickell, E. & Gratzer, W., 1978. Self-Association of Human Spectrin. A Thermodynamic and Kinetic Study. *European Journal of Biochemistry*, 88(2), pp.379–385. Available at: http://doi.wiley.com/10.1111/j.1432-1033.1978.tb12459.x [Accessed May 2, 2015].

Valo, H.K. et al., 2010. Multifunctional hydrophobin: toward functional coatings for drug nanoparticles. *ACS nano*, 4(3), pp.1750–8. Available at: http://dx.doi.org/10.1021/nn9017558 [Accessed May 31, 2015].

Wang, X. et al., 2004. Oligomerization of hydrophobin SC3 in solution: from soluble state to self-assembly. *Protein science : a publication of the Protein Society*, 13(3), pp.810–21. Available at: http://www.pubmedcentral.nih.gov/articlerender.fcgi?artid=2286737&tool=pmcentrez&rendertype=abstract [Accessed May 25, 2015].

Wang, Z. et al., 2010. Mechanisms of protein adhesion on surface films of hydrophobin. *Langmuir : the ACS journal of surfaces and colloids*, 26(11), pp.8491–6. Available at: http://dx.doi.org/10.1021/la101240e [Accessed May 28, 2015].

Vejnovic, I., Simmler, L. & Betz, G., 2010. Investigation of different formulations for drug delivery through the nail plate. *International journal of pharmaceutics*, 386(1-2), pp.185–94. Available at: http://www.ncbi.nlm.nih.gov/pubmed/19941943 [Accessed May 31, 2015].

Wessels, J.G. et al., 1991. The thn mutation of Schizophyllum commune, which suppresses formation of aerial hyphae, affects expression of the Sc3 hydrophobin gene. *Journal of general microbiology*, 137(10), pp.2439–45. Available at: http://www.ncbi.nlm.nih.gov/pubmed/1770359 [Accessed May 23, 2015].

Wessels, J.G.H., 1994. Developmental Regulation of Fungal Cell Wall Formation. *Annual Review of Phytopathology*, 32(1), pp.413–437. Available at: http://www.annualreviews.org/doi/abs/10.1146/annurev.py.32.090194.002213 [Accessed April 19, 2015].

Van Wetter, M.A. et al., 2000. Hydrophobin gene expression affects hyphal wall composition in Schizophyllum commune. *Fungal genetics and biology : FG & B*, 31(2), pp.99–104. Available at: http://www.ncbi.nlm.nih.gov/pubmed/11170739 [Accessed May 23, 2015].

Whiteford, J.R. & Spanu, P.D., 2002. Hydrophobins and the interactions between fungi and plants. *Molecular plant pathology*, 3(5), pp.391–400. Available at: http://www.ncbi.nlm.nih.gov/pubmed/20569345 [Accessed May 24, 2015].

Viterbo, A. & Chet, I., 2006. TasHyd1, a new hydrophobin gene from the biocontrol agent Trichoderma asperellum, is involved in plant root colonization. *Molecular plant pathology*, 7(4), pp.249–58. Available at: http://www.ncbi.nlm.nih.gov/pubmed/20507444 [Accessed May 23, 2015].

De Vocht, M.L. et al., 2002. Self-assembly of the hydrophobin SC3 proceeds via two structural intermediates. *Protein science : a publication of the Protein Society*, 11(5), pp.1199–205. Available at: http://www.pubmedcentral.nih.gov/articlerender.fcgi?artid=2373556&tool=pmcentrez&rendertype=abstract [Accessed May 31, 2015].

De Vries, O.M.H. et al., 1999. Identification and characterization of a tri-partite hydrophobin from Claviceps fusiformis . A novel type of class II hydrophobin. *European Journal of Biochemistry*, 262(2), pp.377–385. Available at: http://doi.wiley.com/10.1046/j.1432-1327.1999.00387.x [Accessed May 31, 2015].

Wösten, H., De Vries, O. & Wessels, J., 1993. Interfacial Self-Assembly of a Fungal Hydrophobin into a Hydrophobic Rodlet Layer. *The Plant cell*, 5(11), pp.1567–1574. Available at: http://www.plantcell.org/content/5/11/1567.abstract [Accessed May 23, 2015].

Wösten, H.A., 2001. Hydrophobins: multipurpose proteins. *Annual review of microbiology*, 55, pp.625–46. Available at: http://www.ncbi.nlm.nih.gov/pubmed/11544369 [Accessed May 23, 2015].

Wösten, H.A. et al., 1994. The fungal hydrophobin Sc3p self-assembles at the surface of aerial hyphae as a protein membrane constituting the hydrophobic rodlet layer. *European journal of cell biology*, 63(1), pp.122–9. Available at: http://www.ncbi.nlm.nih.gov/pubmed/8005099 [Accessed May 23, 2015].

Wösten, H.A. & de Vocht, M.L., 2000. Hydrophobins, the fungal coat unravelled. *Biochimica et biophysica acta*, 1469(2), pp.79–86. Available at: http://www.ncbi.nlm.nih.gov/pubmed/10998570 [Accessed April 19, 2015].

Wösten, H.A.B. et al., 1999. How a fungus escapes the water to grow into the air. *Current Biology*, 9(2), pp.85–88. Available at: http://www.cell.com/article/S0960982299800190/fulltext [Accessed May 23, 2015].

Wösten, H.A.B. & Scholtmeijer, K., 2015. Applications of hydrophobins: current state and perspectives. *Applied microbiology and biotechnology*, 99(4), pp.1587–97. Available at: http://www.ncbi.nlm.nih.gov/pubmed/25564034 [Accessed June 1, 2015].

Yeh, S.R. et al., 1997. Ligand exchange during cytochrome c folding. *Nature structural biology*, 4(1), pp.51–6. Available at: http://www.ncbi.nlm.nih.gov/pubmed/8989324 [Accessed May 26, 2015].

Zampieri, F., Wösten, H.A.B. & Scholtmeijer, K., 2010. Creating Surface Properties Using a Palette of Hydrophobins. *Materials*, 3(9), pp.4607–4625. Available at: http://www.mdpi.com/1996-1944/3/9/4607 [Accessed May 23, 2015].

Zhao, Z.-X. et al., 2007. Amperometric glucose biosensor based on self-assembly hydrophobin with high efficiency of enzyme utilization. *Biosensors & bioelectronics*, 22(12), pp.3021–7. Available at: http://www.sciencedirect.com/science/article/pii/S0956566307000048 [Accessed May 28, 2015].

Zhao, Z.-X. et al., 2009. Self-assembled film of hydrophobins on gold surfaces and its application to electrochemical biosensing. *Colloids and surfaces. B, Biointerfaces*, 71(1), pp.102–6. Available at: http://www.sciencedirect.com/science/article/pii/S0927776509000174 [Accessed May 31, 2015].

Molecular interactions of hydrophobin proteins with their surroundings

Aalto-DD 206/2015
VTT SCIENCE 114

ISBN 978-952-60-6556-4 (printed)
ISBN 978-952-60-6557-1 (pdf)
ISSN-L 1799-4934
ISSN 1799-4934 (printed)
ISSN 1799-4942 (pdf)

978-951-38-8367-6 (printed)
978-951-38-8366-9 (pdf)
2242-119X
2242-119X (printed)
2242-1203 (pdf)

Aalto University
School of Chemical Technology
Department of Biotechnology and Chemical Technology
www.aalto.fi

BUSINESS + ECONOMY

ART + DESIGN + ARCHITECTURE

SCIENCE + TECHNOLOGY

CROSSOVER

DOCTORAL DISSERTATIONS